Biochemistry

pubs.acs.org/biochemistry
Perspective

Light-Driven Enzyme Catalysis: Ultrafast Mechanisms and Biochemical Implications

YongLe He, Marco Barone, Stephen R. Meech, Andras Lukacs, and Peter J. Tonge*

Cite This: *Biochemistry* 2025, 64, 2491−2505
Read Online

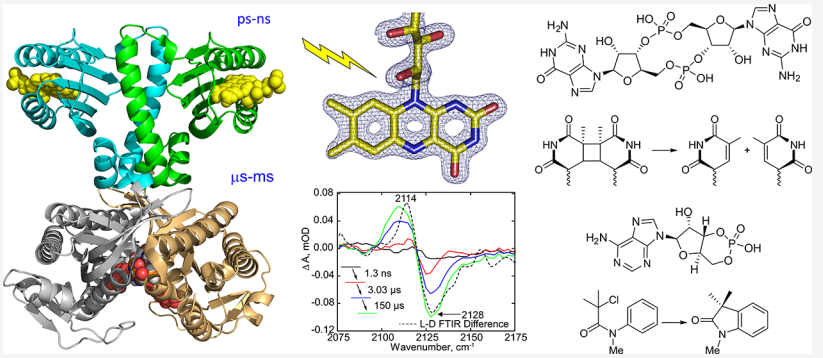

ABSTRACT: Light-activated enzymes are an important class of biocatalysts in which light energy is directly converted into biochemical activity. In most cases the light absorbing group is the isoalloxazine ring of an embedded flavin cofactor and in general two types of mechanism are in operation depending on whether the excited chromophore directly participates in catalysis or where photoexcitation triggers conformational changes that modulate the activity of a downstream output partner. This review will summarize studies on DNA photolyase, fatty acid photodecarboxylase (FAP), the monooxygenase PqsL, and flavin-dependent ene-reductases, where flavin radicals generated by excitation are directly used in the reactions catalyzed by these enzymes, and the blue light using FAD (BLUF) and light oxygen voltage (LOV) domain photoreceptors where flavin excitation drives ultrafast structural changes that ultimately result in enzyme activation. Recent advances in methods such as time-resolved spectroscopy and structural imaging have enabled unprecedented insight into the ultrafast dynamics that underly the mechanism of light-activated enzymes, and here we highlight how understanding ultrafast protein dynamics not only provides valuable insights into natural phototransduction processes but also opens new avenues for enzyme engineering and consequent applications in fields such as optogenetics.

INTRODUCTION

Organisms must adapt to changes in their environment in order to survive and reproduce. This is accomplished through sensory mechanisms that detect stimuli such as light, temperature, and organic molecules. Light sensing is achieved via photoreceptors that control processes such as stress response adaptation, photophobia, phototaxis, photosynthesis, and DNA repair. To understand how light signals are transformed into biological responses and to develop novel light-driven devices, it is essential to study the detailed mechanisms of photoreceptors and determine how ultrafast excitation is coupled to alterations in biological activity on time scales that are many orders of magnitude slower.[1,2]

Ultrafast protein dynamics play a fundamental role in the functionality of light-activated enzymes, facilitating rapid and precise response to photon absorption.[3] These enzymes contain an embedded chromophore and undergo intricate conformational changes upon illumination, triggering cascades of molecular events that culminate in catalytic activation or signal transduction.[4,5] Understanding the ultrafast dynamics that underlie formation of the activated state provides crucial insights into the fundamental mechanisms governing enzyme function and light-driven biological processes. Advanced techniques including time-resolved spectroscopy and femto-second serial crystallography have been applied to elucidate the ultrafast molecular events that control the coupling between light absorption and catalysis in photoactivated enzymes,[3,6,7] which have also been used as model systems to understand how light-triggered ultrafast conformational changes control catalytic reactions in the cell. This review focuses on the ultrafast protein dynamics and activation mechanisms of blue

Received: January 21, 2025
Revised: April 18, 2025
Accepted: April 23, 2025
Published: May 29, 2025

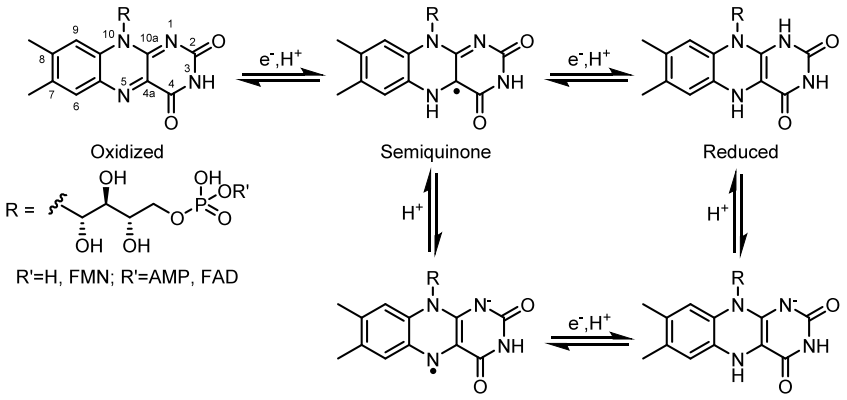

Figure 1. Structures and oxidation states of the flavin chromophore.

light-activated enzymes that utilize an embedded flavin chromophore to absorb light. We do not include light activated enzymes that do not use a flavin such as phytochrome-activated diguanylyl cyclase (PadC)[8] or light-dependent protochlorophyllide reductases.[9]

FLAVIN COFACTORS IN ENZYMES

Flavin cofactors are derived from riboflavin (vitamin B2) and encompass a family of redox-active molecules known for their distinctive chemical properties and biological roles.[10] Flavin cofactors, including flavin mononucleotide (FMN) and flavin adenine dinucleotide (FAD), exist in several oxidation states, each exhibiting unique reactivity and spectral characteristics,[11] and serve as redox carriers, mediating electron transfer reactions, and as functional groups for nucleophilic catalysis and substrate activation (Figure 1).[12]

Light-activated flavin enzymes represent a diverse group of proteins that utilize FAD or FMN as cofactors to initiate photochemical reactions in response to light stimulation. These enzymes play crucial roles in various biological processes, including photoreception, DNA repair, and metabolic regulation.[13] Major classes of light-activated flavin enzymes include DNA photolyase, fatty acid photodecarboxylase (FAP), flavoprotein monooxygenase, and the Blue-Light Utilizing FAD (BLUF) and Light Oxygen Voltage (LOV) sensing domain photoreceptors. In addition, flavin-dependent ene-reductases are an emerging class of light-activated catalysts. The DNA photolyase repairs UV-induced DNA damage including cyclobutane pyrimidine dimers (CPDs) and 6−4 photoproducts (6−4PPs) following visible light excitation of a noncovalently bound FAD cofactor.[14−16] Photolyases are also the evolutionary ancestors of cryptochromes (CRYs) which represent another important class of light-activated flavoproteins, with multiple crucial biological roles in plants and in animals.[17,18] FAP is an enzyme that utilizes blue light to decarboxylate fatty acids, leading to the production of hydrocarbons. The mechanism involves light-induced activation of the enzyme-bound FAD cofactor to initiate fatty acid decarboxylation.[19] PqsL is a monooxygenase from *Pseudomonas aeruginosa* that catalyzes the hydroxylation of aromatic amines during the biosynthesis of 2-alkyl-4-hydroxyquinoline N-oxides (AQNO),[20] while flavin-dependent ene-reductases are versatile catalysts that can be activated by light.[21]

LOV or BLUF light-sensing protein domains contain a flavin chromophore (either FMN or FAD) that triggers light-induced conformational changes in the protein matrix, resulting in downstream signaling events. BLUF and LOV domain photoreceptors are found in various organisms and regulate diverse cellular processes, including phototropism, circadian rhythms, and stress responses.[22,23] Thus, light-activated flavin enzymes catalyze reactions either by stabilizing a highly reducing flavin intermediate that is used directly in the conversion of substrate into product, or by transducing the energy in a photon of light into structural rearrangements that propagate through the protein scaffold, ultimately modulating the activity of a covalently or noncovalently attached output partner. In both cases the molecular events in these processes occur over many decades of time, from the ultrafast subps time scale to the subms time scale.[24]

Ultrafast techniques, such as time-resolved crystallography and femtosecond laser spectroscopy, have emerged as powerful tools for probing the dynamics of light-activated enzymes with unprecedented temporal resolution. In particular, these methods facilitate the capture of transient structural and electronic intermediates and elucidate the sequence of events following photon absorption, shedding light on the molecular choreography underlying enzyme activation and signal transduction pathways.[1,4] In this context, we will provide an overview of the current knowledge regarding ultrafast protein dynamics in light-activated enzymes. We will explore critical examples from the literature, highlighting the structural and functional implications of ultrafast conformational changes in these three classes of enzymes. Additionally, through interdisciplinary approaches combining structural biology, spectroscopy, and computational modeling, we can achieve a deeper insight into the fundamental principles of how biological systems sense and respond to light.

Photolyase: A Light-Activated DNA Repair Enzyme. UV radiation in sunlight can induce the formation of covalent bonds between adjacent pyrimidine bases in DNA, leading to cyclobutane pyrimidine dimers (CPDs) and pyrimidine-pyrimidone 6−4 photoproducts (6−4PPs) which distort the DNA helix and interfere with DNA replication and transcription, potentially leading to mutations and cellular damage.[25] Several systems exist to repair DNA damage including DNA photolyases which are found in plants, fungi, birds, fish, marsupials and some bacteria.[14,26,27] DNA photolyases are members of the photolyase/cryptochrome superfamily which use FAD as the principal light absorbing cofactor and utilize a mechanism known as photoreactivation to repair UV-induced DNA damage.[28,29] Several classes of DNA photolyases have been identified including Class I, II and III CPD photolyases, single-strand specific DNA photolyases, and (6−4) photolyases.[30] Below we summarize aspects of the

https://doi.org/10.1021/acs.biochem.5c00039
Biochemistry 2025, 64, 2491−2505

mechanism of CPD and (6–4) photolyases with particular emphasis on insight gained from ultrafast spectroscopy.

DNA repair by CPD photolyases is initiated by excitation of the reduced anionic state of FAD ($FADH^-$). However, the FAD cofactor in photolyases can also exist in the inactive semireduced radical state FADH*, which must first be converted to $FADH^-$ through a process known as photoactivation.[31] This is achieved by electron transfer from a nearby Trp residue (W382 in *E. coli* photolyase) to the excited state of FADH* (FADH**) which is formed by irradiation of FADH*. W382 is part of a Trp triad that includes W359 and W306 in *E. coli* photolyase which transfers electrons from an exogenous reductant to the FADH** (where * indicates an electronically excited state). Electron transfer through the Trp triad has been studied by ultrafast spectroscopy including polarized femtosecond transient absorption spectroscopy,[32,33] leading to a detailed understanding of electron hopping through the Trp 'wire' (Figure 2).

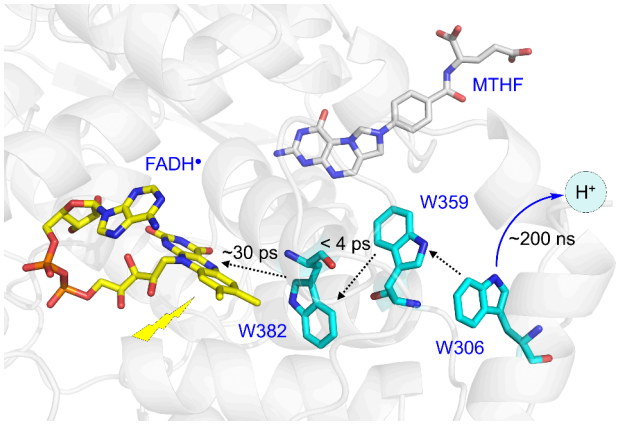

Figure 2. Electron hopping through the Trp triad in DNA photolyase. The electron transfer chain in *E. coli* DNA photolyase. W382 serves as the primary donor to reduce the flavin and the resulting positive charge is stabilized on W306 within 30 ps which then deprotonates in 200 ns. The figure was adapted from Lukacs et al.[33] and was made with PyMOL,[34] from 1DNP.pdb.[35] In addition to the Trp triad, the antenna chromophore 5,10-methenyltetrahydrofolate (MTHF) is also shown.

More recently, femtosecond X-ray crystallography has been used to analyze the structural changes accompanying electron transfer through the Trp chain in the *Drosophila melanogaster* (6–4) photolyase.[36] In *D. melanogaster* photolyase, where the Trp chain consists of 4 Trp residues, the photoexcited cofactor extracts an electron from the proximal Trp residue within just 1 ps, starting the tunneling along the Trp chain, which ultimately results in the formation of a long-range radical pair between $FAD^{\bullet-}$ and the terminal Trp radical. Specific structural dynamics include the Asp397–Arg368 salt bridge which responds within 400 fs to photoreduction of FAD, N403, and reorganization of a water network around the FAD which collectively stabilize the charge on $FAD^{\bullet-}$. The terminal Trp (W381) responds within 20 ps with further dynamics observed for residues around W381 extending to 100 μs, indicating rapid charge transfer followed by structural changes which stabilize the W381 radical. These events are summarized in Figure 3.

DNA repair is initiated by excitation of $FADH^-$ either by direct light absorption or by energy transfer from a light-harvesting antenna chromophore such as 5,10-methenyltetrahydrofolate (MTHF) or 8-hydroxy-7,8-didemethyl-5-deazariboflavin. The antenna chromophore increases the efficiency of catalysis as it has an ∼ 5-fold higher extinction coefficient than the reduced flavin. Following excitation of the antenna, energy is then transferred to the flavin via the classical Förster-type energy transfer mechanism (FRET).[37,38] Using femtosecond fluorescence spectroscopy the fluorescence lifetime of MTHF* in *E. coli* DNA photolyase was 2.6 ns in the absence of an acceptor but was heavily quenched in the presence of the flavin, transferring its energy to $FADH^-$ in 170 ps with an efficiency of ∼ 94%.[39]

Once formed, $FADH^{-}$* transfers an electron to the substrate. Based on ultrafast spectroscopy it has been proposed that electron transfer occurs via the adenine ring of the cofactor which is located between the isoalloxazine ring and the substrate. For the functionally active $FADH^{-}$* redox state this occurs in 2 ns, followed by ultrafast charge recombination in 20 to 700 ps leading to electron tunneling/hopping to the substrate in 200 ps to 6 ns.[29,40,41] Thus, the unique bent conformation of the FAD cofactor is thought to perform a central role in catalysis in which the adenine mediates electron transfer to the substrate.

The reaction catalyzed by the CPD photolyase from *Methanosarcina mazei* (mmCPD) has been studied in detail using time-resolved serial femtosecond crystallography (TR-SFX).[42−44] Maestre-Reyna et al.[42] analyzed the changes in the geometry of the isoalloxazine ring on the ns to μs time scale during the formation of the catalytically active $FADH^-$ state from FAD_{ox} which occurs via two separate electron transfer events separated by a protonation step. This process is mediated by a redox sensor triad comprised of Asn403, Arg378 and Asp409 in which Arg378 is proposed to stabilize the $FAD^{\bullet-}$ formed by the first electron transfer resulting in a twisting of the isoalloxazine ring that is maximized at 300 ns. Subsequently, cleavage of the salt bridge between Arg368–Asp397 enables Arg368 to protonate $FAD^{\bullet-}$ leading to formation of $FADH^{\bullet}$ on the 1–10 μs time-scale followed by a second electron transfer to generate $FADH^-$ which adopts a bent conformation of ∼ 14°.[42]

Subsequently, two research groups published a structural analysis of the reaction catalyzed by mmCPD in complex with the thymine dimer substrate using TR-SFX.[43,44] Christou et al. analyzed the reaction of mmCPD with a *cis-syn* thymine dimer from 3 ps to 30 ns following a 1.1 ps pulse of 396 nm light.[43] This revealed several key features of the reaction coordinate including the observation that the isoalloxazine ring of the cofactor undergoes "butterfly bending" upon excitation resulting in a rearrangement of a hydrogen bond network around the isoalloxazine and adenine rings upon formation of $FADH^{-}$* (within 3 ps) (Figure 4). The change in the water network that interacts with the adenine supports a direct role for the adenine in the electron transfer reaction. Subsequently, on the ps to ns time-scale, the reaction proceeds through the stepwise cleavage of the two carbon–carbon bonds in the thymine dimer via an intermediate in which the C5–C5′ bond is broken, conclusively arguing against a mechanism that involves concerted cleavage of both bonds. During this process, the isoalloxazine ring flattens, assuming a geometry consistent with the $FADH^{\bullet}$ product state. This is followed by product dissociation in 10–100 μs (Figure 4).

Maestre-Reyna et al. also concluded that the reaction was stepwise rather than concerted.[44] This group proposed that the

https://doi.org/10.1021/acs.biochem.5c00039
Biochemistry 2025, 64, 2491−2505

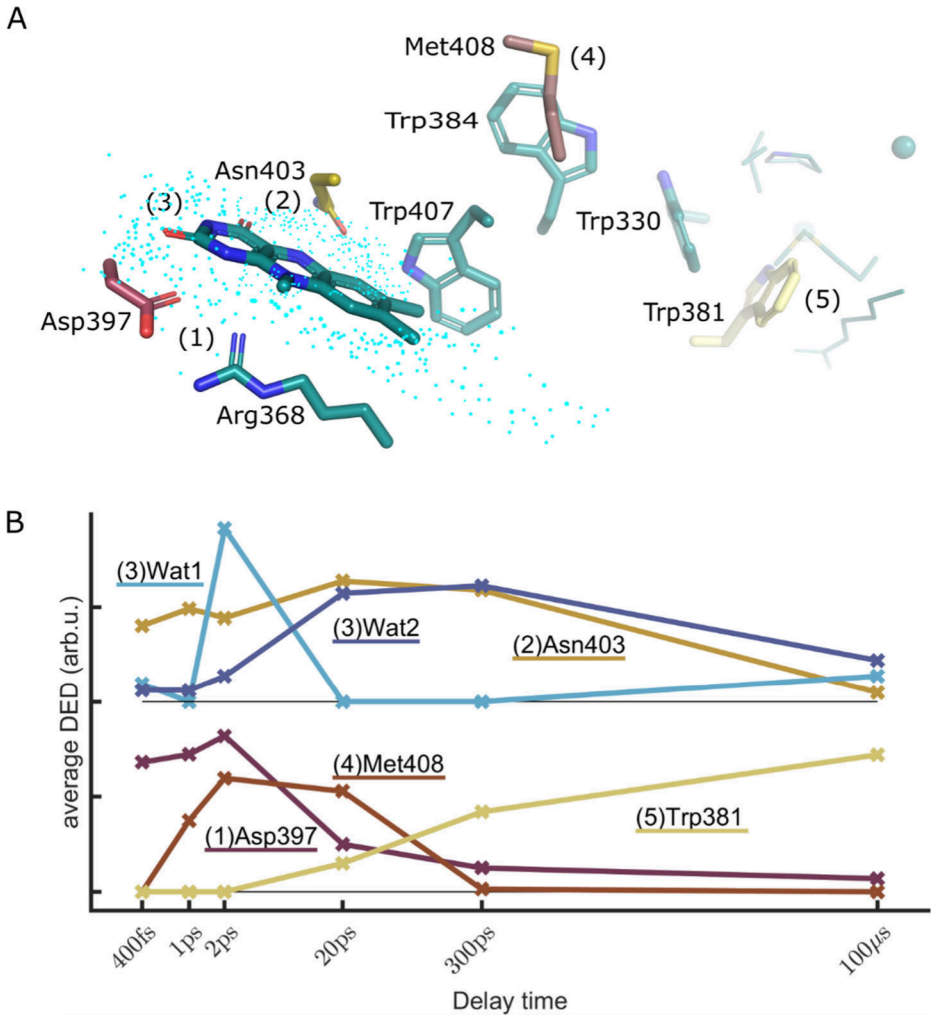

Figure 3. Photochemical events upon reduction of FAD* in *D. melanogaster* (6–4) photolyase. (A) Key residues and processes. (1) FAD is reduced and Asp397 and Arg368 respond immediately. (2) Asn403 reacts similarly fast and undergoes a slow phase of response up to 20 ps. (3) A delayed (from 1 ps) and complex motion of water molecules is completed at 20 ps. (4) Met408 undergoes a photoreaction from 1 to 20 ps. (5) Trp381 is oxidized at 300 ps, with structural changes evolving around it up to 100 μs. (B) The kinetics of the observed difference electron density (DED) at key positions are shown. For water features the electron density is averaged over positive DED > 2σ and for the amino acids over negative DED < 2σ (side chains only). The radius of integration was 2.5 Å. Wat1 corresponds to feature V and Wat2 to feature VI in Figure 3 of Cellini et al.[36] The kinetics for water and Asn403 are vertically offset. The figure was taken from Cellini et al.[36]

electron transfer process from $FADH^-$ to the CPD substrate is initiated by movement of Arg256 in 100 ps, stabilizing the CPD. Following the electron transfer, the cleavage of the C5–C5′ bond of the CPD at ∼ 650 ps leads to formation of a radical anion. Subsequently, at 1 ns, the C6–C6′ bond undergoes cleavage, further advancing the repair reaction. The repair mechanism progresses through different intermediates, transitioning from the CPD radical anion to a pair of thymine bases (Figure 4).

Light-Induced Fatty Acid Decarboxylation. Fatty acid photodecarboxylase (FAP) is an intriguing enzyme that catalyzes the light-driven decarboxylation of fatty acids into hydrocarbons and CO_2, and consequently has important applications in biofuel production.[19] FAP was discovered in microalgae and is a member of the glucose-methanol-choline (GMC) oxidoreductase family.[45] The X-ray structure of the enzyme from *Chlorella variabilis* in complex with palmitate shows that the carboxyl group of the substrate is located close to the isoalloxazine ring of FAD. The reaction was initially characterized using time-resolved fluorescence and absorption spectroscopy resulting in a model in which the excitation of the oxidized FAD results in an excited state (FAD*) that forms $FAD^{\bullet-}$ in ∼ 300 ps due to electron transfer from the substrate, leading to decarboxylation and formation of an alkyl radical.[45] Electron transfer from $FAD^{\bullet-}$ to the alkyl radical was then proposed to result in an alkyl anion in ∼ 100 ns that caused a red shift in the FAD spectrum followed regeneration of the resting state of the enzyme in ∼ 4 ms.[46]

Subsequent serial femtosecond crystallography combined with 100 fs-resolution pump–probe spectroscopy, absorption and Raman microspectrophotometry, FTIR spectroscopy and MD simulations, have provided additional insight in the mechanism of photodecarboxylation.[47] Highlights of these studies include the observation that CO_2 is initially formed with a time constant of ∼ 270 ps i.e. concomitant with electron transfer from substrate to FAD*, and that subsequently dissociation of CO_2 occurs in 100 ns and is accompanied by generation of the oxidized FAD with a red-shifted spectrum. A structure of the product complex is shown in Figure 5 and includes electron density assigned to HCO_3^-, while a proposed

https://doi.org/10.1021/acs.biochem.5c00039
Biochemistry 2025, 64, 2491–2505

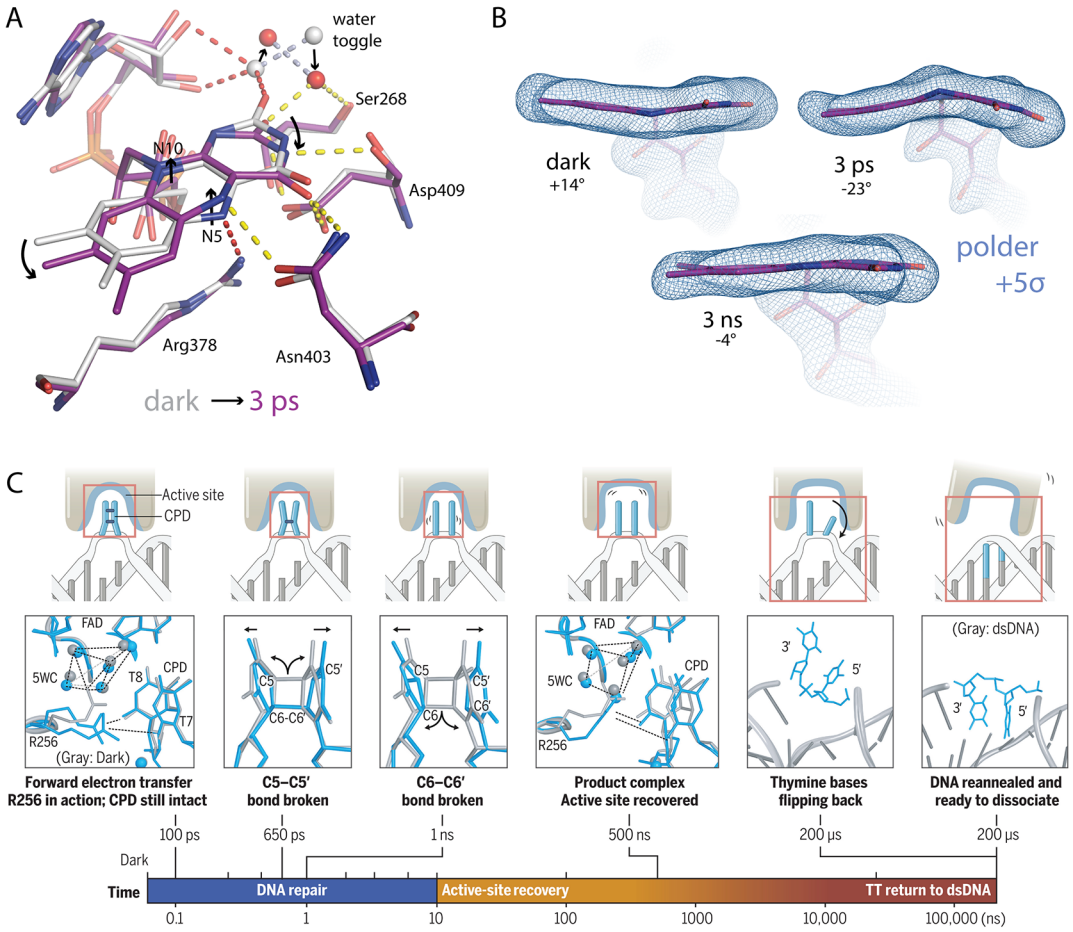

Figure 4. The CPD photolyase reaction mechanism revealed by time-resolved femtosecond crystallography. Structural data of the CPD photolyase from *Methanosarcina maze* (mmCPD) in complex with a synthetic thymine dimer.[43,44] (A) and (B) Excitation of $FADH^-$ results in formation of the $FADH^{-}$* excited state in 3 ps in which the isoalloxazine ring undergoes "butterfly bending" which results in a rearrangement of a hydrogen bond network around the ring that includes amino acid residues and ordered water molecules. This is followed by relaxation of the isoalloxazine ring into the geometry of the $FADH^{\bullet}$ semiquinone product within 3 ns.[43] (C) Key intermediates in the DNA repair reaction catalyzed by photolyase. Selected intermediates (cyan) of the repair process are overlaid with the structure of the dark state (gray) to illustrate structural changes during catalysis. T7 and T8 are the thymine-7 and thymine-8, the damaged 5′- and 3′-thymines of the CPD lesion in the DNA strand. TT refers to the two thymines together.[44] The figure was made from figures in Christou et al.[43] and Maestre-Reyna et al.[44]

photocycle is shown in Figure 6. While a more recent analysis using time-resolved fluorescence and transient absorption proposed that decarboxylation occurs on the ns time-scale,[48] further quantum chemical calculations support a mechanism that involves decarboxylation on the ps time-scale without accumulation of alkyl radical RCOO*.[49,50]

Photoexcitation of FAD to FAD* (1) is followed by electron transfer from the $RCOO^-$ to generate FAD^{*-} in ∼ 300 ps which is accompanied by decarboxylation without accumulation of RCOO* (2). This is followed by electron transfer from FAD^{*-} (presumably to the alkyl radical) in ∼ 100 ns resulting in oxidized FAD with a red-shifted spectrum (FAD_{RS}) which involves proton transfer from an Arg to the alkyl product (3). Concomitantly, most CO_2 (∼75%) is transformed (4) to bicarbonate and FAD_{RS} disappears in ∼ 3 ms (5) with a H/D KIE > 3, indicating coupling to PT. Upon alkane release (6), new substrate binds (7). About 25% of the formed CO_2 is not transformed to bicarbonate, likely because it migrates away from the active site within 100 ns, leaving the protein in ∼ 1.5 µs (4′). In this minor fraction, arginine (R451) should reprotonate at latest in the ∼ 3 ms step (5). Changes after individual steps are marked in red; time constants are for RT. This figure and legend were taken from Figure 8 in Sorigué et al.[47]

The Flavoprotein PqsL from *Pseudomonas aeruginosa*. PqsL is a light activated flavoprotein monooxygenase (FPMO) from *Pseudomonas aeruginosa* where it is involved in the biosynthesis of antibacterial alkyl hydroxyquinoline *N*-oxides (AQNOs).[20] PqsL is a member of the UbiH family and is structurally homologous to group A FPMOs such as p-hydroxybenzoate-3-monooxygenase that have a GSH reductase fold and a nucleotide-binding Rossman fold. PqsL hydroxylates aromatic amines such as 2-aminobenzoylacetate leading to the formation of the respective hydroxyamine. For the reaction to proceed, the bound FAD must be in the fully reduced state which is generated by photoreduction with NAD(P)H. Structural studies support a flavin 'OUT' conformation for the isoalloxazine ring,[51] by analogy to the IN and OUT positions of the ring observed in p-hydroxybenzoate hydroxylase (PHBH).[52] Detailed analysis of the reaction mechanism supports a model for the formation of fully reduced FAD via a two-step mechanism through a single-electron transfer and subsequent semiquinone intermediate (Figure 7). Upon blue-light excitation of the flavin, single

https://doi.org/10.1021/acs.biochem.5c00039
Biochemistry 2025, 64, 2491−2505

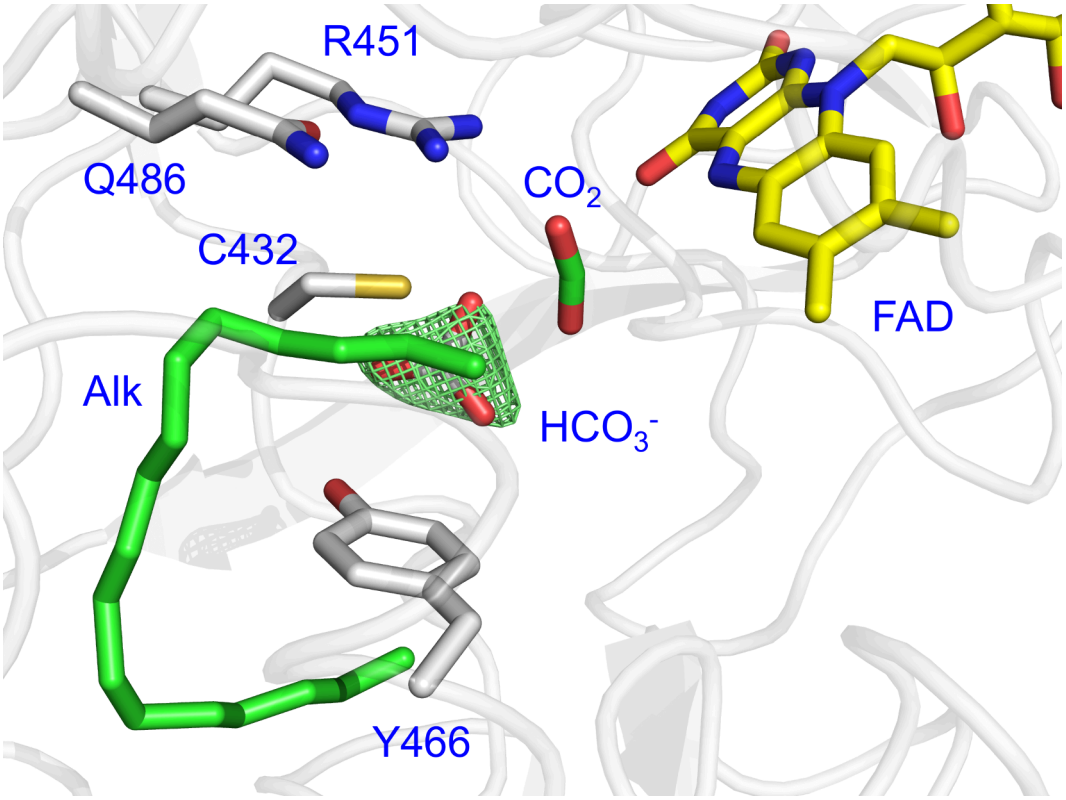

Figure 5. X-ray structure of the FAP product complex. Data were obtained from crystals at 150 K and pH 8.5 and show positive electron density from the polder omit map contoured at 3.5 rmsd, close to C432 that is assigned to bicarbonate (HCO_3^-). Also shown are the alkyl product (Alk), CO_2, and the isoalloxazine ring, which adopts a bent conformation. The figure was made using PyMOL[34] and is adapted from Figure 4D in Sorigué et al.[47]

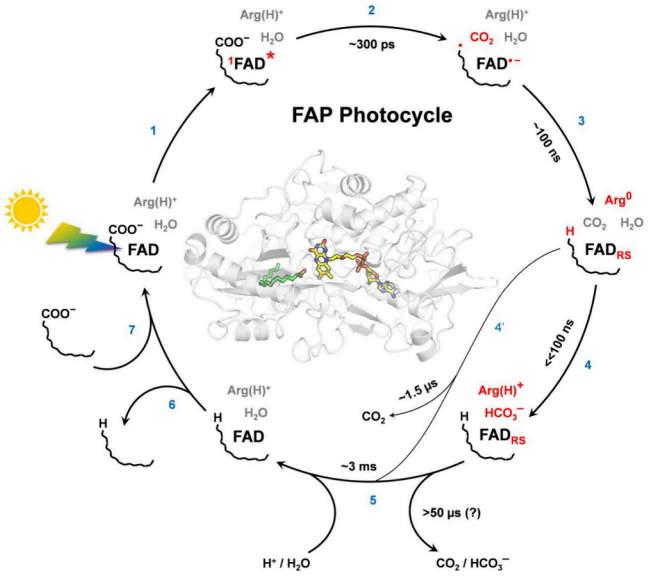

Figure 6. Proposed photocycle for the *C. variabilis* FAP.

electron transfer leads to a transient radical couple between $NADH^{\bullet}$ and $FAD^{\bullet-}$. Rapid protonation prevents accumulation of $FAD^{\bullet-}$ and formation of the fully reduced flavin, $FADH_2$, is proposed to occur by the subsequent disproportionation of two neutral flavin semiquinone species.[51] The current mechanistic studies provide a foundation for the future analysis of the FPMO structural dynamics by ultrafast techniques such as time-resolved crystallography.

Flavin-Dependent Ene-Reductases. Flavin-dependent ene-reductases (EREDs) are versatile biocatalysts, capable of catalyzing stereoselective reactions through hydride transfer or radical mechanisms. EREDs are oxidoreductases that rely on flavin cofactors (FMN or FAD) for their catalytic activity. The first ERED to be discovered was Old Yellow Enzyme, originally isolated from yeast, that utilizes NADPH as the reductant.[53,54] Recent studies have expanded the scope of reactions catalyzed by EREDs by leveraging flavin activation via light excitation.[21] One important application is the photoredox-mediated reduction of aromatic ketones that proceeds via ketyl radical formation. In this process, the flavin is fully reduced by light and then the reduced flavin acts as a hydrogen donor, and supported by ruthenium-based photocatalysts, opens new avenues for non-natural biocatalytic reactions. Mechanistic studies suggest that substrate binding within the enzyme active site lowers the reduction potential, facilitating single electron reduction.[55] For instance, the direct radiation-activation of flavin hydroquinone (FMNhq) in its excited state can lead to the formation of radical intermediates with less reactive substrates, such as α, β-unsaturated amides. This strategy broadens the range of compatible substrates, enhancing catalytic versatility.[55]

One interesting example is the use of flavin-dependent ene-reductases from *Gluconobacter oxidans* (GlueER) to perform cyclization reactions on α-chloroamides. Engineered forms of this enzyme enable improved control of byproducts leading to higher yields and better enantioselectivity.[56] These photoenzymes can perform new reactions such as the light-triggered

https://doi.org/10.1021/acs.biochem.5c00039
Biochemistry 2025, 64, 2491−2505

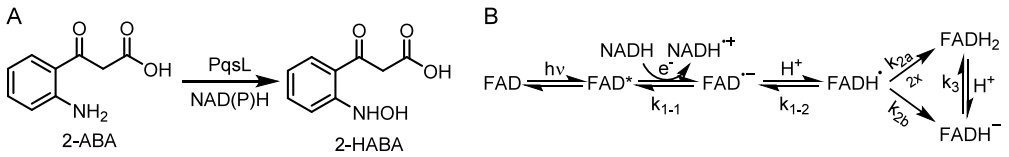

Figure 7. PqsL reaction and proposed mechanism of photoexcitation. (A) PqsL catalyzes the hydroxylation of aromatic amines such as the conversion of 2-aminobenzoylacetate (2-ABA) to 2-hydroxylaminobenzoylacetate (2-HABA). (B) Proposed mechanism for the photoactivation of FAD to $FADH_2$ via the disproportionation of two neutral flavin semiquinone species.[51]

radical cyclization of α-haloamides to oxindoles by 12-oxophytodienoate reductase (OPR1) (Figure 8).[57]

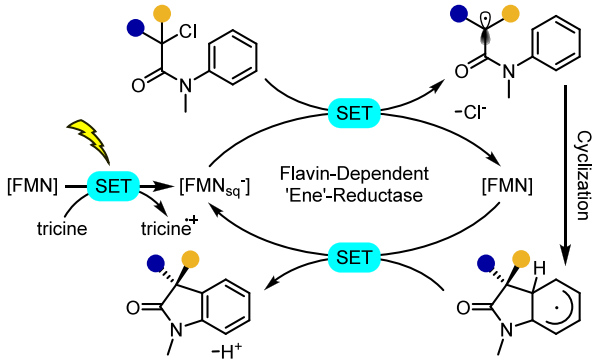

Figure 8. Enzymatic photoreduction of FMN to $FMNsq^-$ (FMN^{*-}). FMN bound to 12-oxophytodienoate reductase (OPR1) is reduced by photoinduced electron transfer to generate $FMNsq^-$. Subsequently, $FMNsq^-$ generates an α-acyl radical which stereoselectively cyclizes to form the oxindole product. SET, single electron transfer. The figure was redrawn based on Black et al.[57]

Light-Activated Enzymes That Generate a Second Messenger. Light-activated enzymes that produce second messengers represent a groundbreaking strategy for dissecting and manipulating cellular signaling networks with unparalleled precision.[58] The unique properties of the light-sensing chromophores allow the modulation of the activity of critical enzymes involved in second messenger synthesis upon light stimulation.[22] This revolutionary approach enables the interrogation of signaling dynamics with high temporal resolution and offers insights into the spatial organization of signaling events within living cells. Light-activated enzymes that produce signaling molecules include the photoactivated adenylate cyclases (PACs), that generate cyclic-AMP (cAMP) from ATP, and photoactivated diguanylate cyclases that synthesize cyclic-di-GMP (c-di-GMP) from two molecules of GTP. Both cAMP and c-di-GMP are important second messengers in cellular signaling pathways, regulating various physiological processes, including gene expression, metabolism, and ion channel activity.[59,60] For instance, the increase in cAMP levels resulting from light activation triggers downstream signaling cascades involving cAMP-dependent protein kinases (PKAs) and other effector proteins,[61] while c-di-GMP is a key regulator of biofilm formation and virulence in bacteria.[62] Finally, PACs are of particular interest in neuroscience and optogenetics as the signaling pathways modulate cellular responses to light stimulation, such as changes in neuronal excitability, synaptic transmission, and gene transcription.[63,64]

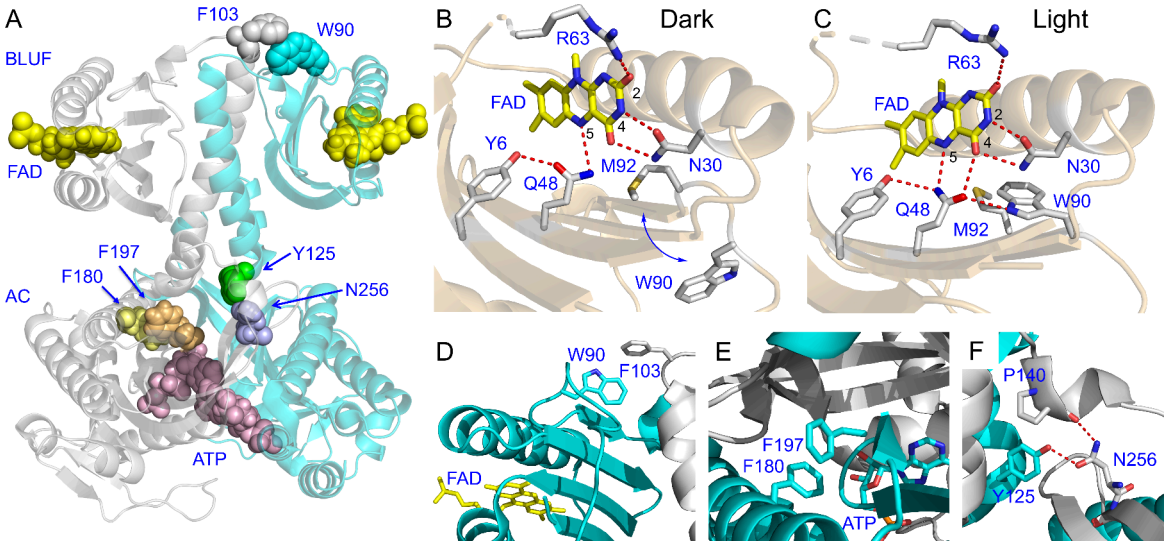

Figure 9. The OaPAC dimer and flavin binding pocket. (A) The OaPAC dimer (PDB: 8QFE). FAD (yellow) and ATP (purple) are shown as spheres in the BLUF and AC domains, respectively. Residues substituted with unnatural amino acids include Y6, W90, F103, Y125, and F180. (B) Dark state of OaPAC with Q48 in the keto tautomer and W90 in the 'OUT' conformation. The Q48 NH_2 is shown hydrogen bonded to the flavin N5 but not the C4 = O. (C) Light state of OaPAC with Q48 rotated and in the enol tautomer, and with W90 adopting the 'IN' conformation. The Q48 enol OH is hydrogen bonded to the flavin C4 = O and accepts a hydrogen bond from the W90 indole NH.[90,91] The movement of W90 is based on the structures of OaPAC determined by serial femtosecond crystallography and cryotrapping (PDB: 8QFE and 8GFG).[92] (D) W90 and F103 were replaced with AzPhe. These residues interact across the dimer interface at the tip of the central helix. (E) F180 was replaced by AzPhe. (F) Y125 was replaced by fluoro-Tyr analogs. Figures (A), (D), (E), and (F) were made using PyMOL[34] and taken/adapted from Jewlikar et al.[93]

https://doi.org/10.1021/acs.biochem.5c00039
Biochemistry 2025, 64, 2491−2505

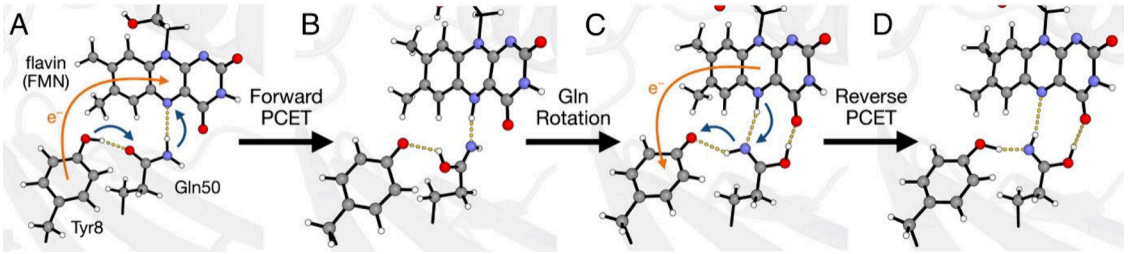

Figure 10. Schematic of the proposed mechanism for the photocycle in the BLUF Slr1694 photoreceptor. (A) The dark-adapted state. Following photoexcitation of the flavin, Tyr8 reduces the flavin to produce a charge-separated state (orange arrow in A), resulting in proton transfer from Tyr8 to the flavin via Gln50 (blue arrows in A) to produce the structure in B. After proton transfer, the Gln50 imidic acid tautomer rotates to form a hydrogen bond with the flavin C4 = O carbonyl, as illustrated by the rotation of Gln50 from B to C. After charge recombination corresponding to electron transfer from the flavin to Tyr8 (orange arrow in C), the proton transfers back from the flavin to Tyr8, again via Gln50 (blue arrows in C) to produce the structure in D, which is the purported light-adapted state with a glutamine imidic acid tautomer. The figure was taken from Goings et al.[90]

BLUF and LOV Domain Photoreceptors. Blue-light using FAD (BLUF) and Light Oxygen Voltage (LOV) domain photoreceptors are widely distributed in bacteria and unicellular eukaryotes,[65] while LOV domains are also found in higher organisms such as plants and fungi.[65−68] Light activated signaling occurs either through noncovalent or covalent interaction with downstream output partners and regulates a variety of biological processes including phototropism, circadian rhythms and gene transcription. Due to their modular structure, the light-absorbing BLUF and LOV domains have been also been used to create novel optogenetic tools.[22,69−74] However, in order to optimize factors such as the dynamic range, quantum yield, lifetime of the photoactivated state and the rates of photoactivation and dark state recovery, a detailed understanding is needed of the photoactivation mechanism, and specifically how ultrafast structural changes on the subps time scale induced by light absorption, lead to macromolecular reorganization and photoreceptor activation on the ms-s time scale. Light-activated enzymes in which the catalytically functional domain is fused to a BLUF or LOV domain are excellent model systems for probing the signal transduction pathway that leads to photoactivation. Enzymes regulated by a BLUF domain include the PACs OaPAC,[75] bPAC from *Beggiatoa*,[63] PACα and PACβ from *Euglena gracilis*,[64] TpPAC from *Turneriella parva*,[76] LiPaC from *Leptonema illini*,[77] nPAC from *Naegleria gruberi*,[78] as well as the phosphodiesterase BlrP1,[79] while those based on a LOV domain include the phototropin serine/threonine kinase,[66,80,81] of which the isolated AsLOV2 domain is the most heavily studied, the diguanylate cyclase LadC, and the senor histidine kinase LOVK,[82] and mPAC from *Microcoleus chthonoplastes*.[83] Below we summarize efforts to determine the mechanism of OaPAC, AsLOV2 and LadC.

The BLUF Photoreceptor OaPAC. OaPAC is a PAC from the photosynthetic cyanobacterium *Oscillatoria acuminata*. The enzyme is a 366-residue homodimer with an N-terminal BLUF domain and a C-terminal class III adenylate cyclase (AC) domain. The two monomers interact in a head-to-head configuration in which the BLUF and AC domains are connected by a coiled coil. Structural studies indicate that the isoalloxazine ring is surrounded by a hydrogen bonding network that includes Y6, Q48 and N30 that are strictly conserved in all BLUF photoreceptors (Figure 9).[65,75] Light absorption results in a 10 nm red shift in the flavin absorbance at 450 nm which is due to a rearrangement of the hydrogen bonding network around the isoalloxazine ring and formation of a second hydrogen bond to the flavin C4 = O.[84,85] Several models have been proposed for the ultrafast perturbation of the conserved hydrogen bond network in BLUF photoreceptors including rotation and/or keto−enol tautomerism of the conserved Gln.[86−89] The prevailing mechanism based on detailed spectroscopic studies including femtosecond stimulated Raman spectroscopy (FSRS) and quantum mechanical/molecular mechanical (QM/MM) molecular dynamics simulations on the related BLUF domain Slr1694/PixD involves rotation and tautomerization of the Gln side chain so that the enol OH forms a hydrogen bond with the C4 = O.[90,91] This model is supported by serial femtosecond crystallography (SFX) and cryo-trapping studies of OaPAC where a rotation of the Q48 side-chain was observed upon photoactivation (Figure 9).[92]

Photoexcitation results in a ∼ 100-fold increase in the synthesis of cAMP from ATP, indicating that adenylate cyclase activity is efficiently suppressed in the dark state.[94] Initial X-ray structural studies of dark and light-adapted OaPAC revealed that the protein does not undergo large scale changes in structure upon photoactivation,[75,95] suggesting that the AC domain must undergo more subtle structural changes to generate the catalytically active state. In addition, based on structural studies using SFX, Chretien et al. proposed that W90 rotates from an 'OUT' conformation in the dark state to an 'IN' conformation in the light state which is accompanied by movement of M92 out of the pocket (Figure 9).[92] This results in the formation of an additional hydrogen bond between Q48 and the indole NH of W90. The movement of W90 alters the position of β-sheet 5 which adopts a new conformation, and causes a restructuring of the loop between β-sheets 4 and 5. Since β-sheet 5 is connected via a loop to α-helix 3 which links the BLUF and AC domains, the light-induced Trp/Met switching is assumed to play a direct role in signal transduction. This proposed movement of W90 in OaPAC is consistent with observations on the related BLUF protein AppA where we used FRET, nanosecond fluorescence anisotropy decay, picosecond fluorescence lifetime measurements and transient IR spectroscopy to show that the analogous Trp (W104) moves from an OUT to an IN conformation during photoactivation.[96]

The OaPAC photoactivation mechanism has also been probed using ultrafast time-resolved infrared spectroscopy (TRIR), time-resolved multiple probe spectroscopy (TRMPS) and transient absorption (TA) spectroscopy coupled with unnatural amino acid mutagenesis. In some BLUF proteins,

https://doi.org/10.1021/acs.biochem.5c00039
Biochemistry 2025, 64, 2491−2505

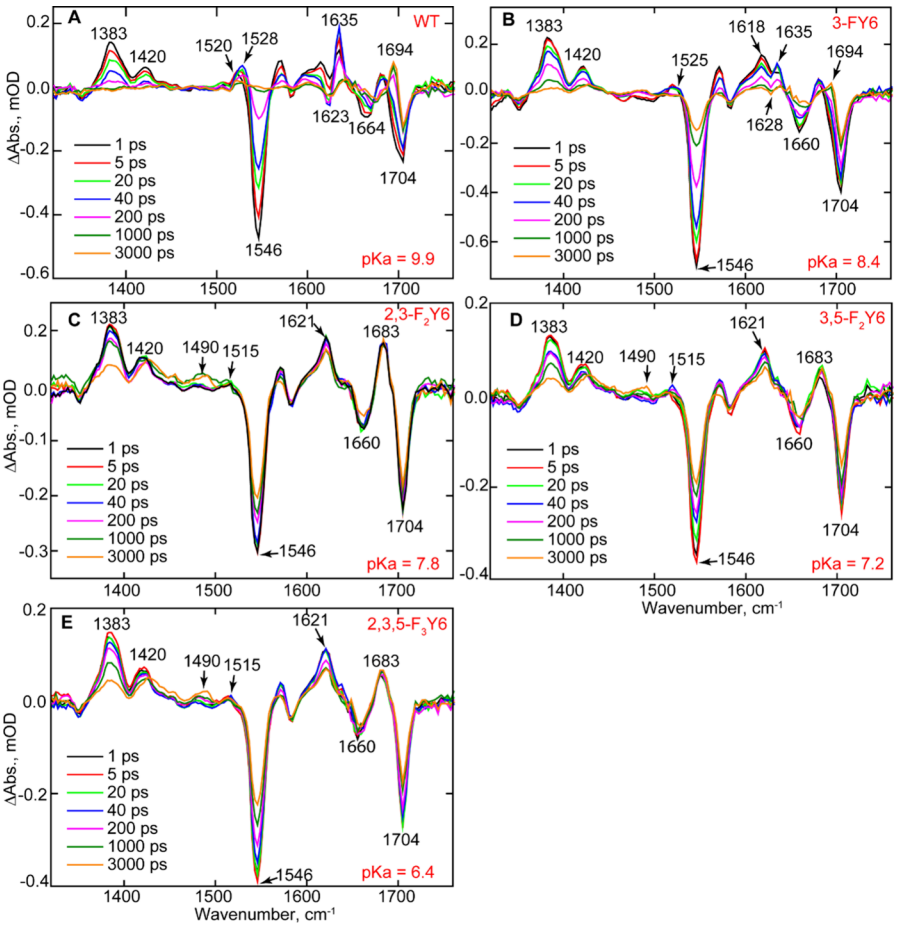

Figure 11. TRIR of wild-type OaPAC and the *n*-FY6 OaPAC variants. Spectra recorded at 1, 5, 20, 40, 200, 1000, and 3000 ps are shown in the figure. (A) Wild-type (WT), (B) 3-FY6, (C) 2,3-F_2Y6, (D) 3,5-F_2Y6, and (E) 2,3,5-F_3Y6. The figure was taken from Tolentino Collado et al.[94]

including OaPAC and Slr1694/PixD, photoexcitation leads to the transient formation of flavin radicals by proton coupled electron transfer (PCET) from the conserved tyrosine (Y6 in OaPAC) to the isoalloxazine ring (Figure 10).[90,91] However, it should be noted that a neutral pathway may exist in some BLUF photoreceptors such as AppA.[97−99]

In OaPAC we investigated the role of Y6 by replacing this residue with fluoro-Tyr analogs that have altered pK_a values and reduction potentials.[94,98,100] TRIR spectra of wild-type OaPAC and variants substituted at position Y6 with 3-fluoroTyr (3-FY6), 2,3-difluoroTyr (2,3-F_2Y6), 3,5-difluoroTyr (3,5-F_2Y6), and 2,3,5-trifluoroTyr (2,3,5-F_3Y6) are shown in Figure 11.

Analysis of the wild-type OaPAC TRIR spectra reveals bands assigned to FAD*$^-$ and FADH* which evolve with the same rate constant, indicating a concerted PCET process. In addition, as the pK_a of the fluoroTyr analogs become more acidic, formation of FADH* is prevented and the photocycle stops at FAD*$^-$ in 2,3-F_2Y6, 3,5-F_2Y6 and 2,3,5-F_3Y6 OaPAC: a transient is observed at 1515 cm^{-1} assigned to FAD*$^-$, however no transients are observed at 1528 cm^{-1} for FADH$^\bullet$ or at 1694 cm^{-1} which is assigned to the FAD C4 = O stretch in the light state. The inability to protonate FAD*$^-$ can be directly linked to photoactivation since enzyme activity is abolished in the most acidic 3,5-F_2Y6 and 2,3,5-F_3Y6 variants (pK_a 7.2 and 6.4, respectively) where the phenol hydroxyl is likely deprotonated. Thus, proton transfer plays an essential role in initiating the structural reorganization of the AC domain that results in enzyme activity.[94] The photocycle deduced from ultrafast spectroscopy together with a summary of the fluoroTyr data are shown in Figure 12.

Fluoro-Tyr substitution has also been used to analyze the importance of an intersubunit hydrogen bond between Y125 and N256 (Figure 9). Y125 is fully conserved in all PACs and is present at the interface between the α3 helix and AC

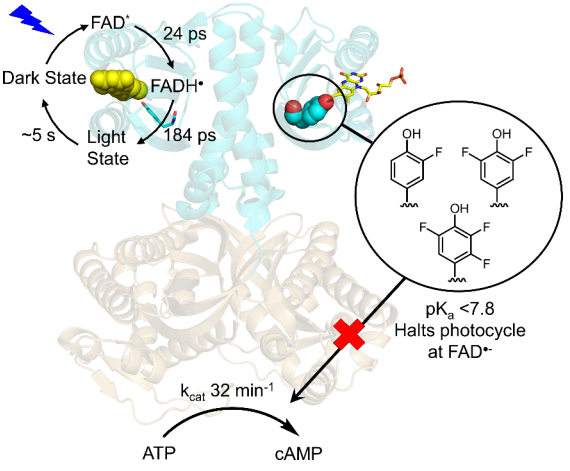

Figure 12. Schematic summary of the OaPAC photocycle and fluoroTyr experiments. The figure was adapted from Tolentino Collado et al.[94]

https://doi.org/10.1021/acs.biochem.5c00039
Biochemistry 2025, 64, 2491−2505

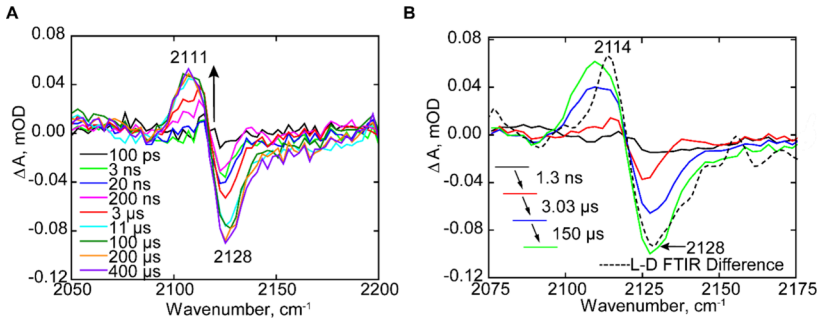

Figure 13. TRMPS spectra of the W90AzPhe OaPAC dark state. (A) Time resolved IR difference response of the azido mode following ultrafast excitation of isoalloxazine cofactor in OaPAC at the W90 position. (B) EADS of W90AzPhe obtained from globally fitting the time-resolved data in A to a sequential first order kinetics model with an initial state (black) two intermediate states (red, blue) which form on a ns−μs time scale, and subsequently relaxes to a final state (green). The final state is compared with the FTIR difference spectra (black dash line). All analyses used the Glotaran software package. The figure was taken from Jewlikar et al.[93]

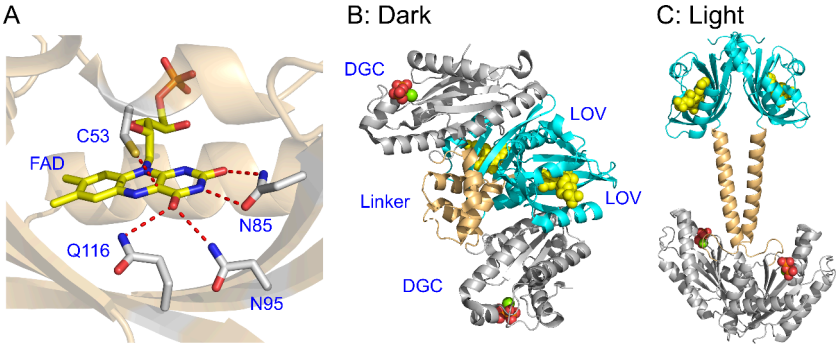

Figure 14. Structure of MsLadC. (A) The flavin binding pocket in the dark state. During photoactivation C53 forms an adduct with the flavin C4a. (B) X-ray structure of dark MsLadC dimer (PDB: 8C05). The BLUF and DGC domains are cyan and gray, and the linker is brown. FAD is yellow and pyrophosphate/Mg^{2+} is colored by atom. (C) The structure predicted by AlphaFold which is thought to be the light activated state.

domain. The Y125F mutant renders both OaPAC, and the related photoreceptor bPAC, catalytically inactive,[75,101] Whereas the light-induced red shift in the FAD spectrum was preserved in all OaPAC variants in which Y125 was replaced with fluoro-Tyr analogs, only 3F−Y125 OaPAC retained light-activated AC activity. In contrast, the 3,5-F_2Y125 and 2,3,5-F_3Y125 photoreceptors were inactive suggesting that Y125 has to be protonated to effectively participate in signal transduction from the BLUF to the AC domains.[93]

The structural dynamics that accompany photoactivation have been explored using the IR reporter azido-Phe (AzPhe) which is a noncanonical amino acid that can be site-specifically incorporated into proteins using the 21st pair/amber codon mutagenesis technique. AzPhe has an intense IR absorption near 2100 cm^{-1} due to the asymmetric stretch of the azide group which falls in a silent region of the protein IR spectrum, so that the band can be unambiguously assigned to the specific AzPhe residue. Although the dependence of the vibrational frequency and band shape on environment is complex,[102] the sensitivity of the band to changes in environment permits the site-specific time-resolution of structural dynamics.[103] AzPhe has previously been used to analyze the dynamics associated with the conserved Trp in the BLUF proteins AppA and PixD.[103] Recently this approach was extended to OaPAC, and AzPhe was incorporated into three positions replacing W90, F103 and F180 (Figure 9). F180 is close to the ATP binding pocket and the F180AzPhe mutant was catalytically inactive. F103 and W90 interact across the dimer interface in the OaPAC dark state. Both F103AzPhe and W90AzPhe had wild-type light-induced catalytic activity, however only W90AzPhe showed a major perturbation in the azido stretching vibration upon photoactivation. Subsequently, TRIR was used time-resolve the structural dynamics of W90AzPhe (Figure 13).

The temporal evolution of the AzPhe at the W90 position shows a negative bleach at 2128 cm^{-1} within ∼ 1 ns and deepens on the μs time scale as a transient at 2111 cm^{-1} evolves (Figure 13). Global analysis resulted in evolution-associated difference spectra (EADS) described by three-time constants of 1.3 ns, 3.03 μs, and 150 μs and a fourth that was kept constant. In contrast to the TRIR of W104AzPhe $AppA_{BLUF}$ and W91AzPhe PixD,[103] no evolution of the W90AzPhe OaPAC azido vibration is detected on the ps time scale. The instantaneous response of the W104AzPhe in AppA and W91AzPhe in PixD was taken as evidence for communication of the AzPhe with the hydrogen bond network surrounding the flavin, i.e. a Trp_{in} conformation, and the absence of an instantaneous perturbation in the spectrum of W90AzPhe is thus consistent with a Trp_{out} conformation in OaPAC.[93]

The LOV Photoreceptor LadC. LadC is a light activated diguanylate cyclase (DGC) in which a LOV domain is coupled to a GGDEF effector domain.[104] The LOV domain, which is a Per-ARNT-Sim (PAS) protein superfamily member, contains a noncovalently bound FMN that is surrounded by a hydrogen bonding network resembling that found in BLUF proteins (Figure 14).[66,81,105−107] Photoactivation results in the formation of an FMN triplet state that subsequently reacts with a conserved Cys to generate a covalent adduct with the C4(a) FMN carbon. This results in a bleach of the 450 nm flavin absorption and appearance of a new band at 390 nm.

https://doi.org/10.1021/acs.biochem.5c00039
Biochemistry 2025, 64, 2491−2505

Vide et al. identified LadC photoreceptors with either short (21 residue) or long (35 residue) linkers between the LOV and DGC domains. Intriguingly, LadCs with short linkers exhibited a 15-fold increase in diguanylate cyclase activity upon activation, whereas the dynamic range for those with longer linkers was >10,000-fold. LOV domains are typically flanked by two helices that are involved in signal transduction, the N-terminal A'α helix and the C-terminal Jα-helix. The structure of LadC from *Methylotenera sp.* (MsLadC), which has a 35-residue linker, was determined in the dark state (Figure 14). The protein is a homodimer with a characteristic LOV-dimer interdomain interface involving the core β-sheet and A'α helices. The Jα-helix often serves as the linker to the effector domain and commonly forms a coiled-coil structure. However, in dark MsLadC the GGDEF domain is folded back onto the LOV domain inhibiting enzyme activity. The conformational dynamics of MsLadC was analyzed using a combination of Size-Exclusion Chromatography with Multi-Angle Light Scattering (SEC-MALS), and hydrogen−deuterium exchange coupled to mass spectrometry (HDX-MS) which supported a major change in structure of the protein upon light activation. In contrast, analogous experiments on LadC from *Aquella Oligotrophica* (AoLadC), which has a short linker, were consistent with similar conformations of this protein in both dark and light states. Based on these data it was proposed that MsLadC undergoes a large-scale conformational change upon photoactivation and adopts the expected elongated coiled-coil structure which was modeled using AlphaFold (Figure 14).[104]

AsLOV2, an Isolated LOV Domain. Phototropins are plant photoreceptors that contain two LOV domains fused to a serine-threonine kinase.[66,108] The isolated LOV2 domain from *Avena sativa* (AsLOV2) has been heavily studied and has been utilized as the light absorbing domain in a variety of optogenetic constructs. AsLOV2 is connected to the kinase domain via the C-terminal Jα-helix, which undergoes structural changes upon light activation leading to dimerization. The allosteric pathways leading to Jα-helix unfolding have been visualized using a combination of TRIR, NMR spectroscopy, MD simulations and in-cell optogenetics which demonstrate the importance of Q513 in the signal transduction pathway and indicate that helix unfolding is complete in ∼ 7 μs Figure 15.[109,110]

The light-induced structural changes in AsLOV2 have also been probed by time-resolved X-ray liquidography (time-resolved X-ray solution scattering, TRXL) which capture the protein structural dynamics directly in solution.[111] TRXL data collected from 5.62 μs to 100−316 ms combined with MD simulations confirmed that the A'α and Jα helices unfold on the microsecond time scale, and that the protein then dimerizes within milliseconds. Experiments with different protein constructs resulted in the conclusion that the dimerization interface involves interaction between the β-scaffolds which is stabilized by local electrostatic interactions. The time-resolved data were then used to propose a kinetic model for photoactivation (Figure 16).

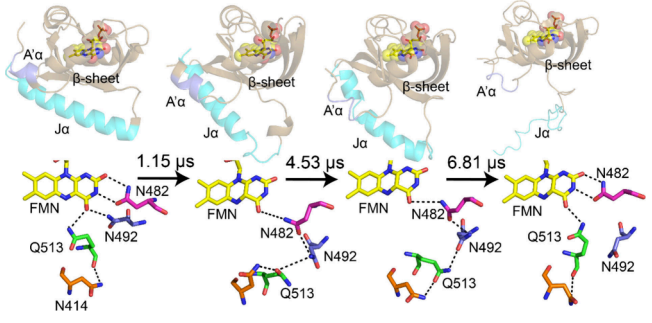

Figure 15. MD simulations of Jα-helix unfolding: The evolution in secondary structure and hydrogen bonding interactions between the flavin and N482, N492, Q513, and N414 for postadduct formation simulation times of 0 (dark state AsLOV2, PDB: 2V1A), 1.15, 4.53, and 6.81 μs (light state, MD). The figure was taken from Iuliano et al.[109]

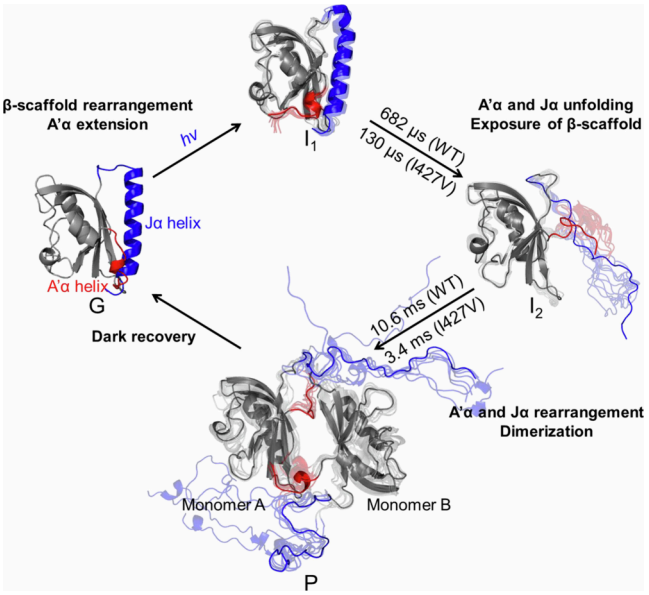

Figure 16. Structural dynamics of the AsLOV2 photocycle revealed by TRXL. The photocycle of AsLOV2 includes the G state, three intermediates (I1, I2, and P), and related time constants (WT: 682 μs and 10.6 ms, and I427V: 130 μs and 3.4 ms), as determined from the kinetic analysis of the scattering data. The optimal structures (I1 and I2) indicate that the structural changes within the A'α and Jα helices allow the exposure of the β-scaffold to the external environment. Subsequently, AsLOV2 undergoes dimerization (P), utilizing the dimeric interface formed between their β-scaffolds. The figure was reproduced from Kim et al.[111]

CONCLUSION

Photoreceptors convert the energy in a photon of light into biological function. To do so they must couple the ultrafast structural changes resulting from the initial photoexcitation into conformational changes that ultimately result in activation of the downstream output partner. Light-activated enzymes, in which the light-absorbing and catalytic domains are part of the same protein, present an unparalleled opportunity to visualize the entire photoactivation pathway and correlate specific structural changes with enzyme activity. This possibility is now being realized with the availability of advanced analytical methods that span multiple time scales enabling the structural dynamics to be resolved in both time and space. In the present review we focus on a subset of systems in which a flavin is the light absorbing chromophore and which demonstrate the detailed structural and mechanistic information that can be extracted using techniques such as ultrafast infrared spectroscopy, transient absorption spectroscopy, serial femtosecond crystallography, time-resolved X-ray solution scattering com-

https://doi.org/10.1021/acs.biochem.5c00039
Biochemistry 2025, 64, 2491−2505

bined with methods such as unnatural amino acid mutagenesis and molecular dynamics simulations. These approaches shed light on the intricate interplay between protein dynamics and function, deepening our understanding of enzymatic mechanisms and paving the way for the design of novel light-driven biocatalysts with applications in the field of optogenetics.

AUTHOR INFORMATION

Corresponding Author

Peter J. Tonge − *Center for Advanced Study of Drug Action and Department of Chemistry, Stony Brook University, Stony Brook, New York 11794, United States; Department of Biomedical Genetics, University of Rochester, Rochester, New York 14642, United States;* orcid.org/0000-0003-1606-3471; Email: peter.tonge@stonybrook.edu

Authors

YongLe He − *Center for Advanced Study of Drug Action and Department of Chemistry, Stony Brook University, Stony Brook, New York 11794, United States*

Marco Barone − *Center for Advanced Study of Drug Action and Department of Chemistry, Stony Brook University, Stony Brook, New York 11794, United States;* orcid.org/0000-0001-7184-2940

Stephen R. Meech − *School of Chemistry, University of East Anglia, Norwich NR4 7TJ, U.K.;* orcid.org/0000-0001-5561-2782

Andras Lukacs − *Department of Biophysics, Medical School, University of Pecs, Pécs 7624, Hungary;* orcid.org/0000-0001-8841-9823

Complete contact information is available at: https://pubs.acs.org/10.1021/acs.biochem.5c00039

Notes

The authors declare no competing financial interest.

ACKNOWLEDGMENTS

This work was supported by grants to P.J.T. from the National Institutes of Health (GM149297) and the National Science Foundation (MCB-1817837) and to S.R.M. from the EPSRC (EP/N033647/1). A.L. acknowledges funding from the Hungarian National Research and Innovation Office (K-137557) and was supported by PTE ÁOK-KA-2021. Y.H. was supported by a National Institutes of Health Chemistry−Biology Interface Training Grant (T32GM092714) and M.B. was supported by an Abroad Fellowship (31189) from Associazione Italiana per la Ricerca sul Cancro (AIRC).

REFERENCES

(1) Seong, J.; Lin, M. Z. Optobiochemistry: Genetically Encoded Control of Protein Activity by Light. *Annu. Rev. Biochem.* **2021**, *90*, 475−501.

(2) Kottke, T.; Xie, A.; Larsen, D. S.; Hoff, W. D. Photoreceptors Take Charge: Emerging Principles for Light Sensing. *Annu. Rev. Biophys* **2018**, *47*, 291−313.

(3) Poddar, H.; Heyes, D. J.; Schiro, G.; Weik, M.; Leys, D.; Scrutton, N. S. A guide to time-resolved structural analysis of light-activated proteins. *FEBS J.* **2022**, *289*, 576−595.

(4) Montgomery, B. L. Sensing the light: photoreceptive systems and signal transduction in cyanobacteria. *Mol. Microbiol.* **2007**, *64*, 16−27.

(5) Fujisawa, T.; Masuda, S. Light-induced chromophore and protein responses and mechanical signal transduction of BLUF proteins. *Biophys Rev.* **2018**, *10*, 327−337.

(6) Greetham, G. M.; Burgos, P.; Cao, Q.; Clark, I. P.; Codd, P. S.; Farrow, R. C.; George, M. W.; Kogimtzis, M.; Matousek, P.; Parker, A. W.; Pollard, M. R.; Robinson, D. A.; Xin, Z. J.; Towrie, M. ULTRA: A Unique Instrument for Time-Resolved Spectroscopy. *Appl. Spectrosc.* **2010**, *64*, 1311−1319.

(7) Hardman, S. J. O.; Iorgu, A. I.; Heyes, D. J.; Scrutton, N. S.; Sazanovich, I. V.; Hay, S. Ultrafast Vibrational Energy Transfer between Protein and Cofactor in a Flavoenzyme. *J. Phys. Chem. B* **2020**, *124*, 5163−5168.

(8) Gourinchas, G.; Etzl, S.; Gobl, C.; Vide, U.; Madl, T.; Winkler, A. Long-range allosteric signaling in red light-regulateddiguanylyl cyclases. *Sci. Adv.* **2017**, *3* (3), n/a.

(9) Gabruk, M.; Mysliwa-Kurdziel, B. Light-Dependent Protochlorophyllide Oxidoreductase: Phylogeny, Regulation, and Catalytic Properties. *Biochemistry* **2015**, *54*, 5255−5262.

(10) Pimviriyakul, P.; Chaiyen, P. Overview of flavin-dependent enzymes. *Enzymes* **2020**, *47*, 1−36.

(11) Kabir, M. P.; Orozco-Gonzalez, Y.; Gozem, S. Electronic spectra of flavin in different redox and protonation states: a computational perspective on the effect of the electrostatic environment. *Phys. Chem. Chem. Phys.* **2019**, *21*, 16526−16537.

(12) Mansoorabadi, S. O.; Thibodeaux, C. J.; Liu, H. W. The diverse roles of flavin coenzymes-nature's most versatile thespians. *J. Org. Chem.* **2007**, *72*, 6329−6342.

(13) Losi, A. Flavin-based Blue-Light photosensors: a photobiophysics update. *Photochem. Photobiol.* **2007**, *83*, 1283−1300.

(14) Sancar, A. Structure and Function of DNA Photolyase and Cryptochrome Blue-LightPhotoreceptors. *Chem. Rev.* **2003**, *103*, 2203−2237.

(15) Emmanuel, M. A.; Bender, S. G.; Bilodeau, C.; Carceller, J. M.; DeHovitz, J. S.; Fu, H.; Liu, Y.; Nicholls, B. T.; Ouyang, Y.; Page, C. G.; Qiao, T.; Raps, F. C.; Sorigue, D. R.; Sun, S. Z.; Turek-Herman, J.; Ye, Y.; Rivas-Souchet, A.; Cao, J.; Hyster, T. K. Photobiocatalytic Strategies for Organic Synthesis. *Chem. Rev.* **2023**, *123*, 5459−5520.

(16) Zhuang, B.; Liebl, U.; Vos, M. H. Flavoprotein Photochemistry: Fundamental Processes and Photocatalytic Perspectives. *J. Phys. Chem. B* **2022**, *126*, 3199−3207.

(17) Mei, Q.; Dvornyk, V. Evolutionary History of the Photolyase/Cryptochrome Superfamily in Eukaryotes. *PLoS One* **2015**, *10*, No. e0135940.

(18) Chaves, I.; Pokorny, R.; Byrdin, M.; Hoang, N.; Ritz, T.; Brettel, K.; Essen, L. O.; van der Horst, G. T.; Batschauer, A.; Ahmad, M. The cryptochromes: blue light photoreceptors in plants and animals. *Annu. Rev. Plant Biol.* **2011**, *62*, 335−364.

(19) Hedison, T. M.; Heyes, D. J.; Scrutton, N. S. Making molecules with photodecarboxylases: A great start or a false dawn? *Curr. Res. Chem. Biol.* **2022**, *2*, 100017.

(20) Drees, S. L.; Ernst, S.; Belviso, B. D.; Jagmann, N.; Hennecke, U.; Fetzner, S. PqsL uses reduced flavin to produce 2-hydroxylaminobenzoylacetate, a preferred PqsBC substrate in alkyl quinolone biosynthesis in Pseudomonas aeruginosa. *J. Biol. Chem.* **2018**, *293*, 9345−9357.

(21) Fu, H.; Hyster, T. K. From Ground-State to Excited-State Activation Modes: Flavin-Dependent "Ene"-Reductases Catalyzed Non-natural Radical Reactions. *Acc. Chem. Res.* **2024**, *57*, 1446−1457.

(22) Losi, A.; Gardner, K. H.; Moglich, A. Blue-Light Receptors for Optogenetics. *Chem. Rev.* **2018**, *118*, 10659−10709.

(23) Lukacs, A.; Tonge, P. J.; Meech, S. R. Photophysics of the Blue Light Using Flavin Domain. *Acc. Chem. Res.* **2022**, *55*, 402−414.

(24) Agarwal, P. K. Enzymes: An integrated view of structure, dynamics and function. *Microb Cell Fact* **2006**, *5*, 2.

(25) Mielko, Z.; Zhang, Y.; Sahay, H.; Liu, Y.; Schaich, M. A.; Schnable, B.; Morrison, A. M.; Burdinski, D.; Adar, S.; Pufall, M.; Van Houten, B.; Gordan, R.; Afek, A. UV irradiation remodels the specificity landscape of transcription factors. *Proc. Natl. Acad. Sci. U. S. A.* **2023**, *120*, No. e2217422120.

(26) Li, Y. F.; Kim, S. T.; Sancar, A. Evidence for lack of DNA photoreactivating enzyme in humans. *Proc. Natl. Acad. Sci. U. S. A.* **1993**, *90*, 4389−4393.

(27) Menck, C. F. Shining a light on photolyases. *Nat. Genet.* **2002**, *32*, 338−339.
(28) Ramirez-Gamboa, D.; Diaz-Zamorano, A. L.; Melendez-Sanchez, E. R.; Reyes-Pardo, H.; Villasenor-Zepeda, K. R.; Lopez-Arellanes, M. E.; Sosa-Hernandez, J. E.; Coronado-Apodaca, K. G.; Gamez-Mendez, A.; Afewerki, S.; Iqbal, H. M. N.; Parra-Saldivar, R.; Martinez-Ruiz, M. Photolyase Production and Current Applications: A Review. *Molecules* **2022**, *27*, 5998.
(29) Zhang, M.; Wang, L.; Zhong, D. Photolyase: Dynamics and Mechanisms of Repair of Sun-Induced DNA Damage. *Photochem. Photobiol.* **2017**, *93*, 78−92.
(30) Kavakli, I. H.; Ozturk, N.; Gul, S. DNA repair by photolyases. *Adv. Protein Chem. Struct Biol.* **2019**, *115*, 1−19.
(31) Weber, S. Light-driven enzymatic catalysis of DNA repair: a review of recent biophysical studies on photolyase. *Biochim. Biophys. Acta* **2005**, *1707*, 1−23.
(32) Aubert, C.; Vos, M. H.; Mathis, P.; Eker, A. P.; Brettel, K. Intraprotein radical transfer during photoactivation of DNA photolyase. *Nature* **2000**, *405*, 586−590.
(33) Lukacs, A.; Eker, A. P.; Byrdin, M.; Brettel, K.; Vos, M. H. Electron hopping through the 15 A triple tryptophan molecular wire in DNA photolyase occurs within 30 ps. *J. Am. Chem. Soc.* **2008**, *130*, 14394−14395.
(34) The PyMOL Molecular Graphics System, Version 2.5. *Schrödinger, LLC*, 2015
(35) Park, H. W.; Kim, S. T.; Sancar, A.; Deisenhofer, J. Crystal structure of DNA photolyase from Escherichia coli. *Science* **1995**, *268*, 1866−1872.
(36) Cellini, A.; Shankar, M. K.; Nimmrich, A.; Hunt, L. A.; Monrroy, L.; Mutisya, J.; Furrer, A.; Beale, E. V.; Carrillo, M.; Malla, T. N.; Maj, P.; Vrhovac, L.; Dworkowski, F.; Cirelli, C.; Johnson, P. J. M.; Ozerov, D.; Stojkovic, E. A.; Hammarstrom, L.; Bacellar, C.; Standfuss, J.; Maj, M.; Schmidt, M.; Weinert, T.; Ihalainen, J. A.; Wahlgren, W. Y.; Westenhoff, S. Directed ultrafast conformational changes accompany electron transfer in a photolyase as resolved by serial crystallography. *Nat. Chem.* **2024**, *16*, 624−632.
(37) Forster, T. Energiewanderung und Fluoreszenz. *Naturwissenschaften* **1946**, *33*, 166−175.
(38) Lakowicz, J. R. *Principles of Fluorescence Spectroscopy*, 3rd ed.; Springer, 2006. DOI: 10.1007/978-0-387-46312-4.
(39) Tan, C.; Guo, L.; Ai, Y.; Li, J.; Wang, L.; Sancar, A.; Luo, Y.; Zhong, D. Direct determination of resonance energy transfer in photolyase: structural alignment for the functional state. *J. Phys. Chem. A* **2014**, *118*, 10522−10530.
(40) Zhang, M.; Wang, L.; Shu, S.; Sancar, A.; Zhong, D. Bifurcating electron-transfer pathways in DNA photolyases determine the repair quantum yield. *Science* **2016**, *354*, 209−213.
(41) Thiagarajan, V.; Byrdin, M.; Eker, A. P.; Muller, P.; Brettel, K. Kinetics of cyclobutane thymine dimer splitting by DNA photolyase directly monitored in the UV. *Proc. Natl. Acad. Sci. U. S. A.* **2011**, *108*, 9402−9407.
(42) Maestre-Reyna, M.; Yang, C. H.; Nango, E.; Huang, W. C.; Ngurah Putu, E. P. G.; Wu, W. J.; Wang, P. H.; Franz-Badur, S.; Saft, M.; Emmerich, H. J.; Wu, H. Y.; Lee, C. C.; Huang, K. F.; Chang, Y. K.; Liao, J. H.; Weng, J. H.; Gad, W.; Chang, C. W.; Pang, A. H.; Sugahara, M.; Owada, S.; Hosokawa, Y.; Joti, Y.; Yamashita, A.; Tanaka, R.; Tanaka, T.; Luo, F.; Tono, K.; Hsu, K. C.; Kiontke, S.; Schapiro, I.; Spadaccini, R.; Royant, A.; Yamamoto, J.; Iwata, S.; Essen, L. O.; Bessho, Y.; Tsai, M. D. Serial crystallography captures dynamic control of sequential electron and proton transfer events in a flavoenzyme. *Nat. Chem.* **2022**, *14*, 677−685.
(43) Christou, N. E.; Apostolopoulou, V.; Melo, D. V. M.; Ruppert, M.; Fadini, A.; Henkel, A.; Sprenger, J.; Oberthuer, D.; Gunther, S.; Pateras, A.; Rahmani Mashhour, A.; Yefanov, O. M.; Galchenkova, M.; Reinke, P. Y. A.; Kremling, V.; Scheer, T. E. S.; Lange, E. R.; Middendorf, P.; Schubert, R.; De Zitter, E.; Lumbao-Conradson, K.; Herrmann, J.; Rahighi, S.; Kunavar, A.; Beale, E. V.; Beale, J. H.; Cirelli, C.; Johnson, P. J. M.; Dworkowski, F.; Ozerov, D.; Bertrand, Q.; Wranik, M.; Bacellar, C.; Bajt, S.; Wakatsuki, S.; Sellberg, J. A.; Huse, N.; Turk, D.; Chapman, H. N.; Lane, T. J. Time-resolved crystallography captures light-driven DNA repair. *Science* **2023**, *382*, 1015−1020.
(44) Maestre-Reyna, M.; Wang, P. H.; Nango, E.; Hosokawa, Y.; Saft, M.; Furrer, A.; Yang, C. H.; Gusti Ngurah Putu, E. P.; Wu, W. J.; Emmerich, H. J.; Caramello, N.; Franz-Badur, S.; Yang, C.; Engilberge, S.; Wranik, M.; Glover, H. L.; Weinert, T.; Wu, H. Y.; Lee, C. C.; Huang, W. C.; Huang, K. F.; Chang, Y. K.; Liao, J. H.; Weng, J. H.; Gad, W.; Chang, C. W.; Pang, A. H.; Yang, K. C.; Lin, W. T.; Chang, Y. C.; Gashi, D.; Beale, E.; Ozerov, D.; Nass, K.; Knopp, G.; Johnson, P. J. M.; Cirelli, C.; Milne, C.; Bacellar, C.; Sugahara, M.; Owada, S.; Joti, Y.; Yamashita, A.; Tanaka, R.; Tanaka, T.; Luo, F.; Tono, K.; Zarzycka, W.; Muller, P.; Alahmad, M. A.; Bezold, F.; Fuchs, V.; Gnau, P.; Kiontke, S.; Korf, L.; Reithofer, V.; Rosner, C. J.; Seiler, E. M.; Watad, M.; Werel, L.; Spadaccini, R.; Yamamoto, J.; Iwata, S.; Zhong, D.; Standfuss, J.; Royant, A.; Bessho, Y.; Essen, L. O.; Tsai, M. D. Visualizing the DNA repair process by a photolyase at atomic resolution. *Science* **2023**, *382*, No. eadd7795.
(45) Sorigue, D.; Legeret, B.; Cuine, S.; Blangy, S.; Moulin, S.; Billon, E.; Richaud, P.; Brugiere, S.; Coute, Y.; Nurizzo, D.; Muller, P.; Brettel, K.; Pignol, D.; Arnoux, P.; Li-Beisson, Y.; Peltier, G.; Beisson, F. An algal photoenzyme converts fatty acids to hydrocarbons. *Science* **2017**, *357*, 903−907.
(46) Heyes, D. J.; Lakavath, B.; Hardman, S. J. O.; Sakuma, M.; Hedison, T. M.; Scrutton, N. S. Photochemical Mechanism of Light-Driven Fatty Acid Photodecarboxylase. *ACS Catal.* **2020**, *10*, 6691−6696.
(47) Sorigué, D.; Hadjidemetriou, K.; Blangy, S.; Gotthard, G.; Bonvalet, A.; Coquelle, N.; Samire, P.; Aleksandrov, A.; Antonucci, L.; Benachir, A.; Boutet, S.; Byrdin, M.; Cammarata, M.; Carbajo, S.; Cuine, S.; Doak, R. B.; Foucar, L.; Gorel, A.; Grunbein, M.; Hartmann, E.; Hienerwadel, R.; Hilpert, M.; Kloos, M.; Lane, T. J.; Legeret, B.; Legrand, P.; Li-Beisson, Y.; Moulin, S. L. Y.; Nurizzo, D.; Peltier, G.; Schiro, G.; Shoeman, R. L.; Sliwa, M.; Solinas, X.; Zhuang, B.; Barends, T. R. M.; Colletier, J. P.; Joffre, M.; Royant, A.; Berthomieu, C.; Weik, M.; Domratcheva, T.; Brettel, K.; Vos, M. H.; Schlichting, I.; Arnoux, P.; Muller, P.; Beisson, F. Mechanism and dynamics of fatty acid photodecarboxylase. *Science* **2021**, *372* (6538), n/a.
(48) Wu, R.; Li, X.; Wang, L.; Zhong, D. Ultrafast Dynamics and Catalytic Mechanism of Fatty Acid Photodecarboxylase. *Angew. Chem., Int. Ed. Engl.* **2022**, *61*, No. e202209180.
(49) Aleksandrov, A.; Bonvalet, A.; Muller, P.; Sorigue, D.; Beisson, F.; Antonucci, L.; Solinas, X.; Joffre, M.; Vos, M. H. Catalytic Mechanism of Fatty Acid Photodecarboxylase: On the Detection and Stability of the Initial Carbonyloxy Radical Intermediate. *Angew. Chem., Int. Ed. Engl.* **2024**, *63*, No. e202401376.
(50) Londi, G.; Salvadori, G.; Mazzeo, P.; Cupellini, L.; Mennucci, B. Protein-Driven Electron-Transfer Process in a Fatty Acid Photodecarboxylase. *JACS Au* **2025**, *5*, 158−168.
(51) Ernst, S.; Rovida, S.; Mattevi, A.; Fetzner, S.; Drees, S. L. Photoinduced monooxygenation involving NAD(P)H-FAD sequential single-electron transfer. *Nat. Commun.* **2020**, *11*, 2600.
(52) Wang, J.; Ortiz-Maldonado, M.; Entsch, B.; Massey, V.; Ballou, D.; Gatti, D. L. Protein and ligand dynamics in 4-hydroxybenzoate hydroxylase. *Proc. Natl. Acad. Sci. U. S. A.* **2002**, *99*, 608−613.
(53) Shi, Q.; Wang, H.; Liu, J.; Li, S.; Guo, J.; Li, H.; Jia, X.; Huo, H.; Zheng, Z.; You, S.; Qin, B. Old yellow enzymes: structures and structure-guided engineering for stereocomplementary bioreduction. *Appl. Microbiol. Biotechnol.* **2020**, *104*, 8155−8170.
(54) Stott, K.; Saito, K.; Thiele, D. J.; Massey, V. Old Yellow Enzyme. The discovery of multiple isozymes and a family of related proteins. *J. Biol. Chem.* **1993**, *268*, 6097−6106.
(55) Sandoval, B. A.; Kurtoic, S. I.; Chung, M. M.; Biegasiewicz, K. F.; Hyster, T. K. Photoenzymatic Catalysis Enables Radical-Mediated Ketone Reduction in Ene-Reductases. *Angew. Chem., Int. Ed. Engl.* **2019**, *58*, 8714−8718.
(56) Biegasiewicz, K. F.; Cooper, S. J.; Gao, X.; Oblinsky, D. G.; Kim, J. H.; Garfinkle, S. E.; Joyce, L. A.; Sandoval, B. A.; Scholes, G.

D.; Hyster, T. K. Photoexcitation of flavoenzymes enables a stereoselective radical cyclization. *Science* **2019**, *364*, 1166−1169.
(57) Black, M. J.; Biegasiewicz, K. F.; Meichan, A. J.; Oblinsky, D. G.; Kudisch, B.; Scholes, G. D.; Hyster, T. K. Asymmetric redox-neutral radical cyclization catalysed by flavin-dependent 'ene'-reductases. *Nat. Chem.* **2020**, *12*, 71−75.
(58) Naim, N.; Reece, J. M.; Zhang, X.; Altschuler, D. L. Dual Activation of cAMP Production Through Photostimulation or Chemical Stimulation. *Methods Mol. Biol.* **2020**, *2173*, 201−216.
(59) Jenal, U.; Reinders, A.; Lori, C. Cyclic di-GMP: second messenger extraordinaire. *Nat. Rev. Microbiol* **2017**, *15*, 271−284.
(60) Popovych, N.; Tzeng, S. R.; Tonelli, M.; Ebright, R. H.; Kalodimos, C. G. Structural basis for cAMP-mediated allosteric control of the catabolite activator protein. *Proc. Natl. Acad. Sci. U. S. A.* **2009**, *106*, 6927−6932.
(61) Yan, K.; Gao, L. N.; Cui, Y. L.; Zhang, Y.; Zhou, X. The cyclic AMP signaling pathway: Exploring targets for successful drug discovery. *Mol. Med. Rep* **2016**, *13*, 3715−3723.
(62) Romling, U.; Galperin, M. Y.; Gomelsky, M. Cyclic di-GMP: the first 25 years of a universal bacterial second messenger. *Microbiol Mol. Biol. Rev.* **2013**, *77*, 1−52.
(63) Stierl, M.; Stumpf, P.; Udwari, D.; Gueta, R.; Hagedorn, R.; Losi, A.; Gartner, W.; Petereit, L.; Efetova, M.; Schwarzel, M.; Oertner, T. G.; Nagel, G.; Hegemann, P. Light modulation of cellular cAMP by a small bacterial photoactivated adenylyl cyclase, bPAC, of the soil bacterium Beggiatoa. *J. Biol. Chem.* **2011**, *286*, 1181−1188.
(64) Iseki, M.; Matsunaga, S.; Murakami, A.; Ohno, K.; Shiga, K.; Yoshida, K.; Sugai, M.; Takahashi, T.; Hori, T.; Watanabe, M. A blue-light-activated adenylyl cyclase mediates photoavoidance in Euglena gracilis. *Nature* **2002**, *415*, 1047−1051.
(65) Gomelsky, M.; Klug, G. BLUF: a novel FAD-binding domain involved in sensory transduction in microorganisms. *Trends Biochem. Sci.* **2002**, *27*, 497−500.
(66) Briggs, W. R.; Christie, J. M.; Salomon, M. Phototropins: a new family of flavin-binding blue light receptors in plants. *Antioxid Redox Signal* **2001**, *3*, 775−788.
(67) Losi, A. The bacterial counterparts of plant phototropins. *Photochem. Photobiol. Sci.* **2004**, *3*, 566−574.
(68) Conrad, K. S.; Manahan, C. C.; Crane, B. R. Photochemistry of flavoprotein light sensors. *Nat. Chem. Biol.* **2014**, *10*, 801−809.
(69) Deisseroth, K. Optogenetics. *Nat. Methods* **2011**, *8*, 26−29.
(70) Moglich, A.; Moffat, K. Engineered photoreceptors as novel optogenetic tools. *Photochem. Photobiol. Sci.* **2010**, *9*, 1286−1300.
(71) Losi, A.; Gartner, W. The evolution of flavin-binding photoreceptors: an ancient chromophore serving trendy blue-light sensors. *Annu. Rev. Plant Biol.* **2012**, *63*, 49−72.
(72) Christie, J. M.; Gawthorne, J.; Young, G.; Fraser, N. J.; Roe, A. J. LOV to BLUF: flavoprotein contributions to the optogenetic toolkit. *Mol. Plant* **2012**, *5*, 533−544.
(73) Shcherbakova, D. M.; Shemetov, A. A.; Kaberniuk, A. A.; Verkhusha, V. V. Natural photoreceptors as a source of fluorescent proteins, biosensors, and optogenetic tools. *Annu. Rev. Biochem.* **2015**, *84*, 519−550.
(74) Zhu, L.; McNamara, H. M.; Toettcher, J. E. Light-switchable transcription factors obtained by direct screening in mammalian cells. *Nat. Commun.* **2023**, *14*, 3185.
(75) Ohki, M.; Sugiyama, K.; Kawai, F.; Tanaka, H.; Nihei, Y.; Unzai, S.; Takebe, M.; Matsunaga, S.; Adachi, S.; Shibayama, N.; Zhou, Z.; Koyama, R.; Ikegaya, Y.; Takahashi, T.; Tame, J. R.; Iseki, M.; Park, S. Y. Structural insight into photoactivation of an adenylate cyclase from a photosynthetic cyanobacterium. *Proc. Natl. Acad. Sci. U. S. A.* **2016**, *113*, 6659−6664.
(76) Penzkofer, A.; Tanwar, M.; Veetil, S. K.; Kateriya, S. Photodynamics of photoactivated adenylyl cyclase TpPAC from the spirochete bacterium Turneriella parva strain H(T). *J. Photochem. Photobiol. B* **2015**, *153*, 90−102.
(77) Penzkofer, A.; Tanwar, M.; Veetil, S. K.; Kateriya, S. Photodynamics of photoactivated adenylyl cyclase LiPAC from the spirochete bacterium Leptonema illini strain 3055. *Trends Appl. Spec* **2014**, *11*, 39−62.
(78) Penzkofer, A.; Stierl, M.; Hegemann, P.; Kateriya, S. Photodynamics of the BLUF domain containing soluble adenylate cyclase (nPAC) from the amoeboflagellate Naegleria gruberi NEG-M strain. *Chem. Phys.* **2011**, *387*, 25−38.
(79) Tyagi, A.; Penzkofer, A.; Griese, J.; Schlichting, I.; Kirienko, N. V.; Gomelsky, M. Photodynamics of blue-light-regulated phosphodiesterase BlrP1 protein from Klebsiella pneumoniae and its photoreceptor BLUF domain. *Chem. Phys.* **2008**, *354*, 130−141.
(80) Christie, J. M.; Salomon, M.; Nozue, K.; Wada, M.; Briggs, W. R. LOV (light, oxygen, or voltage) domains of the blue-light photoreceptor phototropin (nph1): binding sites for the chromophore flavin mononucleotide. *Proc. Natl. Acad. Sci. U. S. A.* **1999**, *96*, 8779−8783.
(81) Crosson, S.; Moffat, K. Structure of a flavin-binding plant photoreceptor domain: insights into light-mediated signal transduction. *Proc. Natl. Acad. Sci. U. S. A.* **2001**, *98*, 2995−3000.
(82) Purcell, E. B.; McDonald, C. A.; Palfey, B. A.; Crosson, S. An analysis of the solution structure and signaling mechanism of LovK, a sensor histidine kinase integrating light and redox signals. *Biochemistry* **2010**, *49*, 6761−6770.
(83) Chen, Z. H.; Raffelberg, S.; Losi, A.; Schaap, P.; Gartner, W. A cyanobacterial light activated adenylyl cyclase partially restores development of a Dictyostelium discoideum, adenylyl cyclase a null mutant. *J. Biotechnol.* **2014**, *191*, 246−249.
(84) Masuda, S.; Hasegawa, K.; Ishii, A.; Ono, T. A. Light-induced structural changes in a putative blue-light receptor with a novel FAD binding fold sensor of blue-light using FAD (BLUF); Slr1694 of synechocystis sp. PCC6803. *Biochemistry* **2004**, *43*, 5304−5313.
(85) Unno, M.; Masuda, S.; Ono, T. A.; Yamauchi, S. Orientation of a key glutamine residue in the BLUF domain from AppA revealed by mutagenesis, spectroscopy, and quantum chemical calculations. *J. Am. Chem. Soc.* **2006**, *128*, 5638−5639.
(86) Stelling, A. L.; Ronayne, K. L.; Nappa, J.; Tonge, P. J.; Meech, S. R. Ultrafast structural dynamics in BLUF domains: transient infrared spectroscopy of AppA and its mutants. *J. Am. Chem. Soc.* **2007**, *129*, 15556−15564.
(87) Udvarhelyi, A.; Domratcheva, T. Photoreaction in BLUF Receptors: Proton-coupled Electron Transfer in the Flavin-Gln-Tyr System. *Photochem. Photobiol.* **2011**, *87*, 554−563.
(88) Domratcheva, T.; Hartmann, E.; Schlichting, I.; Kottke, T. Evidence for Tautomerisation of Glutamine in BLUF Blue Light Receptors by Vibrational Spectroscopy and Computational Chemistry. *Sci. Rep* **2016**, *6*, 22669.
(89) Iwata, T.; Nagai, T.; Ito, S.; Osoegawa, S.; Iseki, M.; Watanabe, M.; Unno, M.; Kitagawa, S.; Kandori, H. Hydrogen Bonding Environments in the Photocycle Process around the Flavin Chromophore of the AppA-BLUF domain. *J. Am. Chem. Soc.* **2018**, *140*, 11982−11991.
(90) Goings, J. J.; Li, P.; Zhu, Q.; Hammes-Schiffer, S. Formation of an unusual glutamine tautomer in a blue light using flavin photocycle characterizes the light-adapted state. *Proc. Natl. Acad. Sci. U. S. A.* **2020**, *117*, 26626−26632.
(91) Hontani, Y.; Mehlhorn, J.; Domratcheva, T.; Beck, S.; Kloz, M.; Hegemann, P.; Mathes, T.; Kennis, J. T. M. Spectroscopic and Computational Observation of Glutamine Tautomerization in the Blue Light Sensing Using Flavin Domain Photoreaction. *J. Am. Chem. Soc.* **2023**, *145*, 1040−1052.
(92) Chretien, A.; Nagel, M. F.; Botha, S.; de Wijn, R.; Brings, L.; Dorner, K.; Han, H.; Koliyadu, J. C. P.; Letrun, R.; Round, A.; Sato, T.; Schmidt, C.; Secareanu, R. C.; von Stetten, D.; Vakili, M.; Wrona, A.; Bean, R.; Mancuso, A.; Schulz, J.; Pearson, A. R.; Kottke, T.; Lorenzen, K.; Schubert, R. Light-induced Trp(in)/Met(out) Switching During BLUF Domain Activation in ATP-bound Photoactivatable Adenylate Cyclase OaPAC. *J. Mol. Biol.* **2024**, *436*, 168439.
(93) Jewlikar, S. S.; Tolentino Collado, J.; Ali, M. I.; Sabbah, A.; He, Y.; Iuliano, J. N.; Hall, C. R.; Adamczyk, K.; Greetham, G. M.; Lukacs, A.; Meech, S. R.; Tonge, P. J. Probing the Signal Transduction

https://doi.org/10.1021/acs.biochem.5c00039
Biochemistry 2025, 64, 2491−2505

Mechanism of the Light-Activated Adenylate Cyclase OaPAC Using Unnatural Amino Acid Mutagenesis. *ACS Chem. Biol.* **2025**, *20*, 369−377.
(94) Tolentino Collado, J.; Iuliano, J. N.; Pirisi, K.; Jewlikar, S.; Adamczyk, K.; Greetham, G. M.; Towrie, M.; Tame, J. R. H.; Meech, S. R.; Tonge, P. J.; Lukacs, A. Unraveling the Photoactivation Mechanism of a Light-Activated Adenylyl Cyclase Using Ultrafast Spectroscopy Coupled with Unnatural Amino Acid Mutagenesis. *ACS Chem. Biol.* **2022**, *17*, 2643−2654.
(95) Ohki, M.; Sato-Tomita, A.; Matsunaga, S.; Iseki, M.; Tame, J. R. H.; Shibayama, N.; Park, S. Y. Molecular mechanism of photoactivation of a light-regulated adenylate cyclase. *Proc. Natl. Acad. Sci. U. S. A.* **2017**, *114*, 8562−8567.
(96) Karadi, K.; Kapetanaki, S. M.; Raics, K.; Pecsi, I.; Kapronczai, R.; Fekete, Z.; Iuliano, J. N.; Collado, J. T.; Gil, A. A.; Orban, J.; Nyitrai, M.; Greetham, G. M.; Vos, M. H.; Tonge, P. J.; Meech, S. R.; Lukacs, A. Functional dynamics of a single tryptophan residue in a BLUF protein revealed by fluorescence spectroscopy. *Sci. Rep* **2020**, *10*, 2061.
(97) He, Y.; Gil, A. A.; Laptenok, S. P.; Fatima, A.; Collado, J. T.; Iuliano, J. N.; Woroniecka, H. A.; Brust, R.; Sabbah, A.; Towrie, M.; Greetham, G. M.; Sazanovich, I. V.; French, J. B.; Lukacs, A.; Meech, S. R.; Tonge, P. J. Enhancing Proton-Coupled Electron Transfer in Blue Light Using FAD Photoreceptor AppA(BLUF). *J. Am. Chem. Soc.* **2025**, *147*, 39−44.
(98) Gil, A. A.; Haigney, A.; Laptenok, S. P.; Brust, R.; Lukacs, A.; Iuliano, J. N.; Jeng, J.; Melief, E. H.; Zhao, R. K.; Yoon, E.; Clark, I. P.; Towrie, M.; Greetham, G. M.; Ng, A.; Truglio, J. J.; French, J. B.; Meech, S. R.; Tonge, P. J. Mechanism of the AppABLUF Photocycle Probed by Site-Specific Incorporation of Fluorotyrosine Residues: Effect of the Y21 pKa on the Forward and Reverse Ground-State Reactions. *J. Am. Chem. Soc.* **2016**, *138*, 926−935.
(99) Lukacs, A.; Brust, R.; Haigney, A.; Laptenok, S. P.; Addison, K.; Gil, A.; Towrie, M.; Greetham, G. M.; Tonge, P. J.; Meech, S. R. BLUF domain function does not require a metastable radical intermediate state. *J. Am. Chem. Soc.* **2014**, *136*, 4605−4615.
(100) Gil, A. A.; Laptenok, S. P.; Iuliano, J. N.; Lukacs, A.; Verma, A.; Hall, C. R.; Yoon, G. E.; Brust, R.; Greetham, G. M.; Towrie, M.; French, J. B.; Meech, S. R.; Tonge, P. J. Photoactivation of the BLUF Protein PixD Probed by the Site-Specific Incorporation of Fluorotyrosine Residues. *J. Am. Chem. Soc.* **2017**, *139*, 14638−14648.
(101) Lindner, R.; Hartmann, E.; Tarnawski, M.; Winkler, A.; Frey, D.; Reinstein, J.; Meinhart, A.; Schlichting, I. Photoactivation Mechanism of a Bacterial Light-Regulated Adenylyl Cyclase. *J. Mol. Biol.* **2017**, *429*, 1336−1351.
(102) Lee, H.; Choi, J. H.; Cho, M. Vibrational solvatochromism and electrochromism of cyanide, thiocyanate, and azide anions in water. *Phys. Chem. Chem. Phys.* **2010**, *12*, 12658−12669.
(103) Hall, C. R.; Tolentino Collado, J.; Iuliano, J. N.; Gil, A. A.; Adamczyk, K.; Lukacs, A.; Greetham, G. M.; Sazanovich, I.; Tonge, P. J.; Meech, S. R. Site-Specific Protein Dynamics Probed by Ultrafast Infrared Spectroscopy of a Noncanonical Amino Acid. *J. Phys. Chem. B* **2019**, *123*, 9592−9597.
(104) Vide, U.; Kasapovic, D.; Fuchs, M.; Heimbock, M. P.; Totaro, M. G.; Zenzmaier, E.; Winkler, A. Illuminating the inner workings of a natural protein switch: Blue-light sensing in LOV-activated diguanylate cyclases. *Sci. Adv.* **2023**, *9*, No. eadh4721.
(105) Nash, A. I.; Ko, W. H.; Harper, S. M.; Gardner, K. H. A conserved glutamine plays a central role in LOV domain signal transmission and its duration. *Biochemistry* **2008**, *47*, 13842−13849.
(106) Nozaki, D.; Iwata, T.; Ishikawa, T.; Todo, T.; Tokutomi, S.; Kandori, H. Role of Gln1029 in the photoactivation processes of the LOV2 domain in adiantum phytochrome3. *Biochemistry* **2004**, *43*, 8373−8379.
(107) Harper, S. M.; Neil, L. C.; Gardner, K. H. Structural basis of a phototropin light switch. *Science* **2003**, *301*, 1541−1544.
(108) Christie, J. M. Phototropin Blue-Light Receptors. *Ann. Rev. Plant Biol.* **2007**, *58*, 21−45.
(109) Iuliano, J. N.; Collado, J. T.; Gil, A. A.; Ravindran, P. T.; Lukacs, A.; Shin, S.; Woroniecka, H. A.; Adamczyk, K.; Aramini, J. M.; Edupuganti, U. R.; Hall, C. R.; Greetham, G. M.; Sazanovich, I. V.; Clark, I. P.; Daryaee, T.; Toettcher, J. E.; French, J. B.; Gardner, K. H.; Simmerling, C. L.; Meech, S. R.; Tonge, P. J. Unraveling the Mechanism of a LOV Domain Optogenetic Sensor: A Glutamine Lever Induces Unfolding of the Jalpha Helix. *ACS Chem. Biol.* **2020**, *15*, 2752−2765.
(110) Gil, A. A.; Laptenok, S. P.; French, J. B.; Iuliano, J. N.; Lukacs, A.; Hall, C. R.; Sazanovich, I. V.; Greetham, G. M.; Bacher, A.; Illarionov, B.; Fischer, M.; Tonge, P. J.; Meech, S. R. Femtosecond to Millisecond Dynamics of Light Induced Allostery in the Avena sativa LOV Domain. *J. Phys. Chem. B* **2017**, *121*, 1010−1019.
(111) Kim, C.; Yun, S. R.; Lee, S. J.; Kim, S. O.; Lee, H.; Choi, J.; Kim, J. G.; Kim, T. W.; You, S.; Kosheleva, I.; Noh, T.; Baek, J.; Ihee, H. Structural dynamics of protein-protein association involved in the light-induced transition of Avena sativa LOV2 protein. *Nat. Commun.* **2024**, *15*, 6991.

https://doi.org/10.1021/acs.biochem.5c00039
Biochemistry 2025, 64, 2491−2505